1989

Incorporation of nonlinear load models and identification of the inter-area mode phenomenon in the transient energy function method

Neelu Gopal Bhatia
Iowa State University

INFORMATION TO USERS

The most advanced technology has been used to photograph and reproduce this manuscript from the microfilm master. UMI films the text directly from the original or copy submitted. Thus, some thesis and dissertation copies are in typewriter face, while others may be from any type of computer printer.

The quality of this reproduction is dependent upon the quality of the copy submitted. Broken or indistinct print, colored or poor quality illustrations and photographs, print bleedthrough, substandard margins, and improper alignment can adversely affect reproduction.

In the unlikely event that the author did not send UMI a complete manuscript and there are missing pages, these will be noted. Also, if unauthorized copyright material had to be removed, a note will indicate the deletion.

Oversize materials (e.g., maps, drawings, charts) are reproduced by sectioning the original, beginning at the upper left-hand corner and continuing from left to right in equal sections with small overlaps. Each original is also photographed in one exposure and is included in reduced form at the back of the book. These are also available as one exposure on a standard 35mm slide or as a 17" x 23" black and white photographic print for an additional charge.

Photographs included in the original manuscript have been reproduced xerographically in this copy. Higher quality 6" x 9" black and white photographic prints are available for any photographs or illustrations appearing in this copy for an additional charge. Contact UMI directly to order.

U·M·I

University Microfilms International
A Bell & Howell Information Company
300 North Zeeb Road, Ann Arbor, MI 48106-1346 USA
313/761-4700 800/521-0600

Order Number 9003503

Incorporation of nonlinear load models and identification of the inter-area mode phenomenon in the transient energy function method

Bhatia, Neelu Gopal, Ph.D.

Iowa State University, 1989

U·M·I
300 N. Zeeb Rd.
Ann Arbor, MI 48106

Incorporation of nonlinear load models and identification of the inter-area mode phenomenon in the transient energy function method

by

Neelu Gopal Bhatia

A Dissertation Submitted to the
Graduate Faculty in Partial Fulfillment of the
Requirements for the Degree of
DOCTOR OF PHILOSOPHY

Department: Electrical Engineering and Computer Engineering
Major: Electrical Engineering (Electric Power)

Approved:

Signature was redacted for privacy.

In Charge of Major Work

Signature was redacted for privacy.

For the Major Department

Signature was redacted for privacy.

For the Graduate College

Members of the Committee:

Signature was redacted for privacy.

Iowa State University
Ames, Iowa
1989

TABLE OF CONTENTS

LIST OF TABLES

LIST OF FIGURES

1 INTRODUCTION

The term "stability" refers to that property which ensures that the power system will remain in operating equilibrium under normal and abnormal operating conditions. Power system stability has become an area of concern as power systems over large geographic areas have been interconnected and power systems have grown in size and have become more complex. Over the last two decades, considerable research effort has gone into the stability investigation of power systems, especially after the famous blackout in Northeast U.S.A. in 1965. With the ever increasing demand for electrical energy and dependence on an uninterrupted supply, the associated requirement of high reliability dictates that power systems be designed to maintain stability under specific disturbances. The first requirement of reliable service is to keep the synchronous generators running in parallel and with adequate capacity to meet the load demand. A second requirement of reliable electrical service is to maintain the integrity of the power network.

Transient stability studies are concerned with the stability characteristics of the electric power system under large disturbances, which may be a sudden change in load, or a sudden change in reactances of the system caused, for instance, by a line outage or a fault. The nature and magnitude of these disturbances greatly affect the stability of the system. A power system is transiently stable for a particular

steady-state operating condition and for a particular disturbance if, following that disturbance, it reaches an acceptable steady-state operating condition.

1.1 Need for Direct Methods of Transient Stability Analysis

Transient stability studies are conducted on power systems to analyze the effect of large disturbances. One of the important objectives of such studies is to evaluate the ability of power systems to withstand contingencies for decision making, which range from minute-to-minute operations to planning decisions for the future. This involves ascertaining whether the existing or planned switchgear and network arrangements are adequate for the system to withstand a prescribed set of disturbances without loss of synchronism being encountered. Another emerging need of power system operation deals with obtaining the stability limits for various planned or forced equipment outages under changing operating conditions. These stability limits of interest can, for instance, be in terms of power generation of an economic unit or power transfer across certain critical interfaces of the transmission system. Given these safe limits, the system operator, would take necessary actions to remain within these limits to avoid any stability crisis. Fast computation of stability limits thus requires a dependable analytical technique, which should be fast enough to provide answers in or near real-time.

The conventional method to analyze transient stability is to obtain a time solution of the equations describing the power system. These equations consist of a set of differential and algebraic equations, which are usually solved by a digital computer simulation. These simulations suffer from two main drawbacks. Firstly, time simulations consume enormous computing resources and engineering time, and,

secondly, they do not provide a qualitative measure of the degree of stability of the power system.

Direct methods on the other hand, offer alternative methods which are aimed at relaxing the technical and economical burdens associated with the time solution approach. In addition, direct methods provide information regarding relative degree of stability of different operating configuration for a system. For system operation with forced outage of lines, these methods can provide stable operating regimes in near real time. In operations planning, these methods identify problem contingencies and define safe regimes at a reduced cost. In system planning, these methods are useful in weighting alternative expansion plans, according to the relative network strength to withstand contingencies.

It is because of these technical and economical reasons that the need for the direct methods of transient stability assessment arose. The direct methods in turn should predict transient stability (or instability) of a power system reliably, when subjected to a given disturbance, and provide a quick assessment of transient stability at a reduced cost.

The direct stability analysis based on the transient energy function (TEF) method is a potential candidate to meet the requirements of real time transient stability evaluation. The main features that make the TEF method an attractive candidate for fast computation of stability limits are the avoidance of time consuming step-by-step time domain simulations and provisions for qualitative measure of the degree of system stability via the energy margin.

1.2 Basis for the Transient Energy Function Method

The second method of Lyapunov provides the theoretical origin of the direct methods. Successful application of the direct methods requires the construction of a valid Lyapunov function and the determination of the region of stability. Many of the Lyapunov functions used are selected on the basis of energy considerations and they are called energy functions.

The second or "direct" method of Lyapunov is based on a basic concept. The principal idea is contained in the following reasoning

> "*If the rate of change* $\frac{dE}{dt}$ *of the energy* $E(\underline{x})$ *of an isolated physical system is negative for every possible state* $\underline{x}$ *except for a single equilibrium state* $\underline{x}_e$*, then the energy will continually decrease until it finally assumes its minimum value* $E(\underline{x}_e)$" [1].

The concept of the TEF method can be easily understood by a simple analogy. Consider a vehicle being pushed uphill, as in Figure 1.1. The point at which the vehicle rests at the bottom of the hill is referred to as the stable equilibrium point (SEP). Motion is initiated in the vehicle by giving it a sudden push, transferring to it some energy, V.

This disturbance causes an imbalance and injects energy into the system. This makes the vehicle move away from equilibrium. The energy components can clearly be identified as kinetic and potential. The maximum amount of energy, V_{max}, that could be given to the vehicle without it going over the hill can be easily computed. The point at which this maximum energy is achieved (the top of the hill) is the unstable equilibrium point (UEP). The sign of $\Delta V = V_{max} - V$ indicates whether

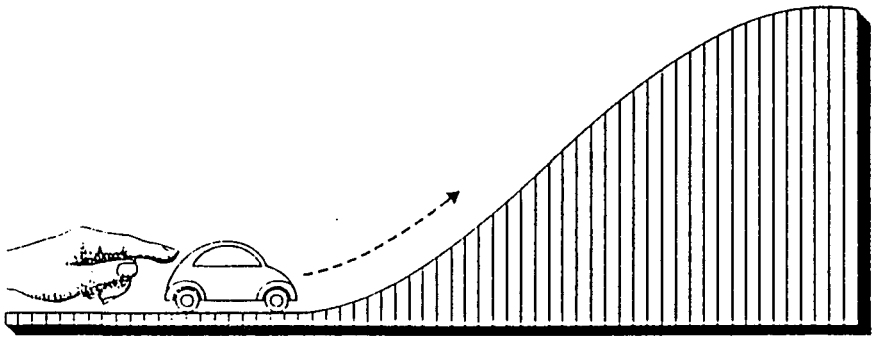

Figure 1.1: The vehicle-hill analogy

or not the vehicle will go over the hill, and the magnitude of ΔV indicates how much additional energy could have been given to the vehicle without it going over the hill. On the other hand, if the sign is negative , the vehicle will go over the hill, and the magnitude of ΔV indicates how much less energy should have been given to the vehicle so that it would not have gone over the hill [2]. In other words, in the post disturbance period, the kinetic energy must be converted to potential energy if stability is to be maintained.

Similarly, when a power system's equilibrium is disturbed, there is an excess (or deficiency) of energy associated with the synchronous machines, setting the machines to move away from equilibrium. This motion is indicative of the fact that the excess energy is converted to kinetic energy (or the energy deficiency is extracted from the kinetic energy of the rotating masses). If that motion goes on indefinitely, synchronism would be lost. To avoid this, the system must be capable of absorbing this excess energy at a time when the forces on the generators tend to bring the generators back toward new equilibrium positions. This capability depends on the potential energy of the post disturbance network. For a given post disturbance system configuration, there is a maximum or critical amount of transient energy that the network can absorb. Thus, requirements of a good transient stability assessment are functions that describe the transient energy responsible for the separation of one or more generators from the rest of the system, and a good estimate of the critical energy required for the generators to lose synchronism with the system.

The TEF method adopts the center of inertia (COI) formulation, which describes the motion of all generators with respect to the inertial center. This formulation offers physical insight into the transient stability problem and also removes

the energy associated with the inertial center acceleration which does not contribute to the stability determination. The energy function which accounts for the transient energy of the system is computed with respect to the energy at the equilibrium state of the post disturbance network. The transient energy function has two components: kinetic energy and potential energy.

1.3 Transient Stability Assessment

In the TEF method, the transient stability assessment is made by comparing two values of the system transient energy function V. The value of V at the end of a disturbance,V^{cl}, is compared with a critical value of V, which is V^{cr}, the potential energy at the controlling UEP. If V^{cl} is less than V^{cr} the system is stable and if V^{cl} is greater than V^{cr} the system is unstable. It is obvious that if correct and reliable assessment is to be achieved, accurate and reliable evaluation of both values of V must be made. This in turn implies a reliable evaluation of the SEP and UEP, the conditions at the end of the disturbance, and an accurate accounting of the transient energy.

1.4 Review of Direct Methods of Transient Stability Analysis

1.4.1 Early work on energy functions

The earlier work on the development of direct methods for the transient stability analysis of power systems involved energy methods. The earliest and most familiar energy method for transient stability analysis is an "equal area criterion" for a single machine-infinite bus system. This criterion simply states that if the ki-

netic energy acquired by the generator rotor during the disturbed period is less than, or equal to, the energy converted to potential energy during the post disturbance state, then stability will be maintained. Kimbark [3] gives a detailed treatment of this subject.

In 1930, Gorev (in the Soviet Union) used the first integral of energy to obtain a criterion for power system stability for a 3-machine system [4]. This criterion used a solution method equivalent to the determining of a region of stability for the SEP. This was one of the earliest energy function method and was not discovered in the West until the 1970s.

In 1947, Magnusson [5] applied the energy function to determine the stability of a power system. He developed a technique using the classical model with zero transfer conductances. His approach was very similar to Gorev's. However, the significant difference between these two formulations was that Magnusson derived the energy function with respect to the post disturbance SEP.

In 1958, Aylett [6] proposed an "energy integral criterion" for multimachine systems. He studied the nature of phase-plane trajectories of a multimachine system using the classical model and arrived at the criterion for stability based on the comparison of the phase-plane trajectories with a critical trajectory which passes through a saddle point. The most significant aspect of this work is the formulation of the system equations based on the inter-machine movements. The concept of the "separatrix" and "region of stability" was also introduced in this paper.

1.4.2 Application of Lyapunov's direct method

After this early work on energy methods, Lyapunov's direct method emerged as a solution to the power system stability problem. The pioneering work in this area was done by Gless [7] and El-Abiad and Nagappan [8]. Gless [7] used a single machine infinite bus example and matched the results obtained by direct method to those obtained by using equal area criterion and Aylett's phase-plane technique. In 1966, El-Abiad and Nagappan [8] developed a Lyapunov function for a multimachine power system.

A great deal of attention was devoted by the researchers toward identification of correct critical energy levels. In essence, it involved identifying an appropriate UEP among numerous UEP solutions existing in a multimachine system. Gupta and El-Abiad [9] identified that the UEP of least potential energy may not be near the trajectory at all, and it may lead to very conservative results. With the explanation based on system behavior, the relevant UEP was identified as the one with minimum energy levels among the UEPs close to the disturbed trajectory. Thus the exact determination of the UEP closest to the disturbed trajectory and reduction in search time are the main contributions of this work.

Since then, a great deal of research effort has been devoted to the systematic construction of Lyapunov's function for transient stability analysis of power systems, and determination of region of stability for these functions. The survey papers by Fouad [10] and Ribbens-Pavella [11] provide a comprehensive review of the work done in this area until the mid 1970s.

Stability analysis by Lyapunov theory gave very conservative results when compared to conventional time simulation, and appeared to be a mere academic exercise

and was viewed with skepticism by the power industry.

1.4.3 Improvements to the Direct Methods

The approach of formulating the system equations with respect to the system inertial center [12,13] improved the calculation of transient energy. The inertial center formulation removes the component of system transient energy that does not contribute to instability, namely, the energy that accelerates the inertial center. Further, this formulation enables the analyst to draw an analogy between each machine of a multimachine system and the one machine infinite bus system.

In the late 1970s, attention was again focussed on developing a suitable energy function which could be expressed in terms of physical energy components.

In 1979, Athay and co-workers [14,15] at Systems Control, Inc. (SCI) made significant progress towards developing the TEF method for practical applications. These accomplishments are summarized below:

1. A clear understanding and verification of the fact that by appropriately accounting for fault location, the stability of a multimachine system can be assessed. This played a vital role in the identification of the relevant UEP.

2. The development of techniques for the direct determination of critical clearing times. Approximate method of incorporating the effects of transfer conductances, accurate fault-on trajectory approximation and calculation of UEPs.

3. The concept of the potential energy boundary surface (PEBS), developed by Kakimoto and co-workers [16], using a Lur'e type Lyapunov function, was utilized to understand the system separation mechanism, which allowed for

significant improvements in direct stability assessment.

As with the previous methods, this still had drawbacks in terms of providing conservative results for the critical clearing time for a wide range of fault conditions. In certain cases with a complex mode of instability, the correct unstable equilibrium point (UEP) could not be predicted accurately.

For an accurate estimate of the region of stability, extensive simulations were conducted by Fouad and co-workers [17,18] at Iowa State University and the conclusions of these simulations provided the physical insight into the modes of instability of a practical power system. Among their findings were the following:

1. Not all the excess kinetic energy at the instant of fault-clearing contributes directly to the separation of the critical machines from the rest of the system. This component of kinetic energy which accounts for the other intermachine swings should be subtracted from the energy that needs to be absorbed by the system for stability to be maintained.

2. When more than one generator tends to lose synchronism, instability is determined by the gross motion of these machines, i.e., by the motion of their center of inertia.

3. The concept of a controlling UEP for a particular system trajectory is a valid concept.

The identification and the actual calculation of the controlling UEP in the absence of time solutions is a challenging task. Fouad et al. [19] developed a criterion to identify a controlling UEP among several probable candidate UEPs

provided by the analyst. The criterion provided by them accounts for two important aspects of the transient behavior of the systems, namely,

- the effect of disturbance on various generators, and
- the energy absorbing capacity of the post disturbance network.

Pai [1] summarizes various methods of computing the region of stability in a systematic manner. Chiang et al. [20] presented a theoretical foundation for the direct method by providing a mathematical and physical reasoning for the existence of the controlling UEP.

In 1982, Vittal [21] and Michel et al. [22] developed an individual machine energy function in order to identify the transient energy pulling a particular machine from the rest of the system. Michel et al. [22] have concluded that system separation does not depend on the total system energy, but rather on the transient energy of individual machines or groups of machines. However, the individual machine energies along the faulted trajectories need to be evaluated at each time step, thus increasing the computation time.

With these significant contributions, the TEF method became a reliable technique for assessing transient stability. Over the recent years, the TEF method has been extended by improving computation techniques and modeling of power system components. These improvements include applications of the TEF method to stressed large-scale power systems [23,24], incorporation of the effects of exciter [25,26], 2 terminal HVDC [26] and out-of-step impedance relays [27].

1.5 Motivation for the Present Work

Although the importance of the behavior of loads as a function of voltage in power system stability studies has long been recognized, and studies of load characteristics have been made many years ago, except for rather special cases, stability was usually regarded as a problem of holding the generators together [28] and hence the emphasis was on refinements of generator representation, with the loads regarded as secondary.

However, this situation has changed, and much more attention has been devoted to load behavior as a function of both voltage and frequency within the last decade. There are several reasons for this:

1. The tendency to improve the quantitative accuracy of system simulation
2. The study of large interconnected systems, which makes it necessary to have a certain consistency in representation among the component systems.

Considerable progress has been made in first swing power system transient stability assessment using the TEF method. Recently, the technique has also been successfully applied to large-scale power systems. The technique has also been tested on a variety of applications. In most of the work reported in the literature, the technique has been applied to the classical power system model. This research attempts to remove some of the modeling restrictions of the TEF method by incorporating the effect of nonlinear load models.

In some earlier work on incorporation of nonlinear load models, the PEBS method was used to estimate the critical energy [29,30,31]. In [29], real and reactive loads at each bus are represented as voltage-dependent functions of a base demand.

The demand term is represented as a torque, and a conceptual swing equation is developed for each load bus. The energy corresponding to each load bus is then added to the energy corresponding to the machine swing equations to obtain total system energy.

In [30], current injections corresponding to the load buses are reflected at the internal generator buses under the assumption that the complex ratio of the internal generator voltage to the load bus voltage is constant.

In [31], the sparse formulation using the PEBS is used to represent the nonlinear loads. Since a time simulation is made to obtain the trajectory, an alternate network solution is done at each time instant to obtain the voltages at the load buses, maintaining the nonlinear characteristic.

This research outlines in detail a procedure to represent nonlinear load models; including combinations of constant current and constant MVA components, in the reduced TEF formulation. The effect of the nonlinear loads on the SEP and the controlling UEP solutions are determined via current injections of load components during the solution process at the internal generator nodes. The energy function is suitably modified to account for these current injections. A procedure is proposed to conduct transient stability assessment using the new energy function.

The other aspect of this research deals with the application of the TEF method to stressed large-scale power systems. The advent of extensive interconnected operation and the inability of the utilities to install additional transmission capacity has led to the maximum loading of transmission lines in certain regions.

In many parts of the network the stressed conditions are created by:

- a high level of system loading,

- heavy power transfers across certain transmission interfaces and
- heavy loading of certain plants for economic operation.

Under these stressed conditions the power system is vulnerable to disturbances that can affect reliability.

When the area of stress encompasses most of the interconnected system, the system has to be represented in its entirety. In such cases, geographically remote disturbances can have an effect upon the other portions of the system. Moreover, it may be necessary to identify exactly the key areas that separate from the system in extreme situations.

The post disturbance network of the stressed system is characterized by weak synchronizing forces caused by large transmission impedances. The generators away from the fault location may also separate from the system. The dynamic phenomenon can be described as follows: Following the disturbance, a small group of generators close to the fault location are severely disturbed initially. But, as the transient progresses, the weak synchronizing forces in the system dominate. When instability occurs, it takes place as a separation of a large group of generators (including the small group severely disturbed by the fault initially) from the rest of the system. This is the so-called "inter-area" mode phenomenon of stressed systems. In extreme situations of instability, the post disturbance network, with loss of critical transmission facility, may not even be steady-state stable. The stability limited conditions of interest in operating the stressed systems (e.g., power transfer across a critical transmission interface) may be limited by the power generation levels of units far away from the fault location.

Hence, we need some technique which would identify the possibility of the inter-area mode phenomenon. The technique suggested in this research work uses the theory of modal analysis to identify the inter-area mode.

1.6 Scope of this Research Work

The objectives of this research work are:

1. Develop a technique to account for the effects of nonlinear loads in the TEF method.
2. Apply this technique to a 4-generator test system and a 17-generator test system.
3. Compare the results obtained by this technique with those obtained by time simulation.
4. Develop a technique which would identify the possibility of the inter-area mode phenomenon.
5. Apply this technique to several test systems, including stressed and unstressed systems.
6. Indicate the inter-area mode, if present.

2 MATHEMATICAL MODEL

2.1 System Equations

The simplest model representing a multi-machine power system, commonly called the classical model in literature [32] has been used in the analysis presented below. This model is based on the following assumptions:

1. Mechanical power input to each generator remains constant.
2. Damping is negligible.
3. The synchronous machine can be represented by a constant voltage source behind transient reactance.
4. The motion of the rotor of the machine coincides with the angle of the voltage behind transient reactance.
5. Loads are represented by constant shunt impedances.

It should be noted that the last assumption is not applied to Chapter 3, where the loads are represented by constant current or constant MVA.

Based on these assumptions, the swing equations that govern the dynamics of the n-machine system are given by

$$\begin{aligned} M_i\dot{\omega}_i &= P_i - P_{ei} \\ \dot{\delta}_i &= \omega_i\ , \qquad\qquad i = 1,2,\ldots,n \end{aligned} \tag{2.1}$$

where

$$\begin{aligned} P_i &= P_{mi} - E_i^2 G_{ii} \\ P_{ei} &= \sum_{\substack{j=1 \\ j\neq i}}^{n} [C_{ij}\sin(\delta_i - \delta_j) + D_{ij}\cos(\delta_i - \delta_j)] \\ C_{ij} &= E_i E_j B_{ij}, \quad D_{ij} = E_i E_j G_{ij} \end{aligned}$$

and

G_{ii} - driving point conductance

P_{mi} - mechanical power input

E_i - internal bus voltage of generator i

M_i - inertia constant

$G_{ij} + jB_{ij}$ - the transfer admittance in the system reduced to the internal node between generators i and j

ω_i, δ_i - generator rotor speed and angle deviations with respect to a synchronously rotating reference frame

The above equations are written with respect to an arbitrary synchronously rotating reference frame. Transforming equations (2.1) into the inertial reference frame, provides a better physical insight into the transient stability problem formulation. This formulation conveniently removes the kinetic energy associated with the acceleration of the inertial center of the system [18].

In order to transform equations (2.1) to the center of inertia (COI) frame, define

$$\begin{aligned} M_T &\equiv \sum_{i=1}^{n} M_i \\ \delta_0 &\equiv \frac{1}{M_T} \sum_{i=1}^{n} M_i \delta_i \end{aligned} \tag{2.2}$$

Then

$$\begin{aligned} \omega_0 &= \dot{\delta}_0 \\ M_T \dot{\omega}_0 &= \sum_{i=1}^{n} M_i \dot{\omega}_i = \sum_{i=1}^{n} (P_i - P_{ei}) \equiv P_{COI} \end{aligned} \tag{2.3}$$

Now, the new angle and speed of machine i in COI frame is

$$\theta_i \equiv \delta_i - \delta_0$$

$$\tilde{\omega}_i \equiv \omega_i - \omega_0$$

It can be noted that $\underline{\theta}$ and $\underline{\tilde{\omega}}$ always satisfy the constraints of the inertial center reference frame, namely,

$$\begin{aligned} \sum_{i=1}^{n} M_i \theta_i &= 0 \\ \sum_{i=1}^{n} M_i \tilde{\omega}_i &= 0 \end{aligned} \tag{2.4}$$

In the inertial center reference frame, the equations of motion become

$$\begin{aligned} M_i \dot{\tilde{\omega}}_i &= P_i - P_{ei} - \frac{M_i}{M_T} P_{COI} = f_i \\ \dot{\theta}_i &= \tilde{\omega}_i \,, \qquad i = 1, 2, \ldots, n \end{aligned} \tag{2.5}$$

2.2 Equilibrium Points

The equilibrium points of the system are the points which satisfy

$$\begin{aligned} 0 &= P_i - P_{ei} - \frac{M_i}{M_T} P_{COI} \\ 0 &= \tilde{\omega}_i \quad i = 1, 2, \ldots, n \end{aligned} \tag{2.6}$$

From these equilibrium points, the stable equilibrium point (SEP) $\underline{\theta}^s$ and the controlling unstable equilibrium point (UEP) $\underline{\theta}^u$ are of interest for the analysis by the TEF method. The SEP will have all generator angles less than $\pi/2$ radians. The calculation of $\underline{\theta}^s$ is rather straightforward, as it represents the unique post disturbance steady state operating condition. The unstable equilibrium points can be as many as a theoretical maximum of $2^{n-1} - 1$ for a n-machine system [1]. The controlling UEP $\underline{\theta}^u$ is the unstable equilibrium point relevant to the disturbance under investigation. This represents the unstable equilibrium point of the system, in which the angles of a certain group of generators are advanced (generally, greater than $\pi/2$ radians, in the case where the disturbance causes the generators to accelerate).

The mode of disturbance (MOD) is a terminology for characterizing the controlling UEP. The controlling UEP can be described by a certain group of machines severely affected by the disturbance; they include, but are not necessarily restricted to the machines initially losing synchronism in the post disturbance network [17]. The group of machines characterizing the controlling UEP is referred to as the MOD for a given disturbance and a specific post disturbance network.

2.3 The Transient Energy Function in the COI Formulation

From the system equations (2.5), the transient energy function V is given by [18]

$$V = \frac{1}{2}\sum_{i=1}^{n} M_i\tilde{\omega}_i^2 - \sum_{i=1}^{n} P_i(\theta_i - \theta_i^s) - \sum_{i=1}^{n-1}\sum_{j=i+1}^{n}[C_{ij}(\cos\theta_{ij} - \cos\theta_{ij}^s) - \int_{\theta_i^s+\theta_j^s}^{\theta_i+\theta_j} D_{ij}\cos\theta_{ij}\,d(\theta_i+\theta_j)] \quad (2.7)$$

where $\underline{\theta}^s$ is the SEP of the post disturbance system.

The first term in equation (2.7) is the kinetic energy while the other terms represent the rotor position energy, magnetic energy and the dissipation energy components, respectively of the system potential energy. The last term, which represents the energy dissipated in the network transfer conductances is a path-dependent integral. This term can be calculated only if the system trajectory is known. For the purpose of analysis by the direct method, this term has been approximated with linear approximation of the trajectory.

Chapter 3 will demonstrate how the nonlinear load models can be incorporated in the TEF method, and Chapter 4 will illustrate the results of this modeling.

3 INCORPORATION OF NONLINEAR LOAD MODELS IN THE TEF METHOD

3.1 General Approach

In detailing the approach in incorporating the nonlinear loads in the TEF method, it is convenient to take an overview of the various steps involved in the basic TEF procedure [24]. Figure 3.1 outlines the various algorithmic steps in the TEF procedure.

Careful analysis of the various steps in the TEF procedure indicates that there are four major components, in which the effect of nonlinear loads have to be incorporated. These are:

1. SEP and UEP solution
2. Conditions at fault clearing
3. Mode of disturbance (MOD) evaluation
4. Energy margin computation

The main idea is to reflect the load current vector onto the generator internal buses. In the following sections, the details of the nonlinear load incorporation in each of the components will be discussed.

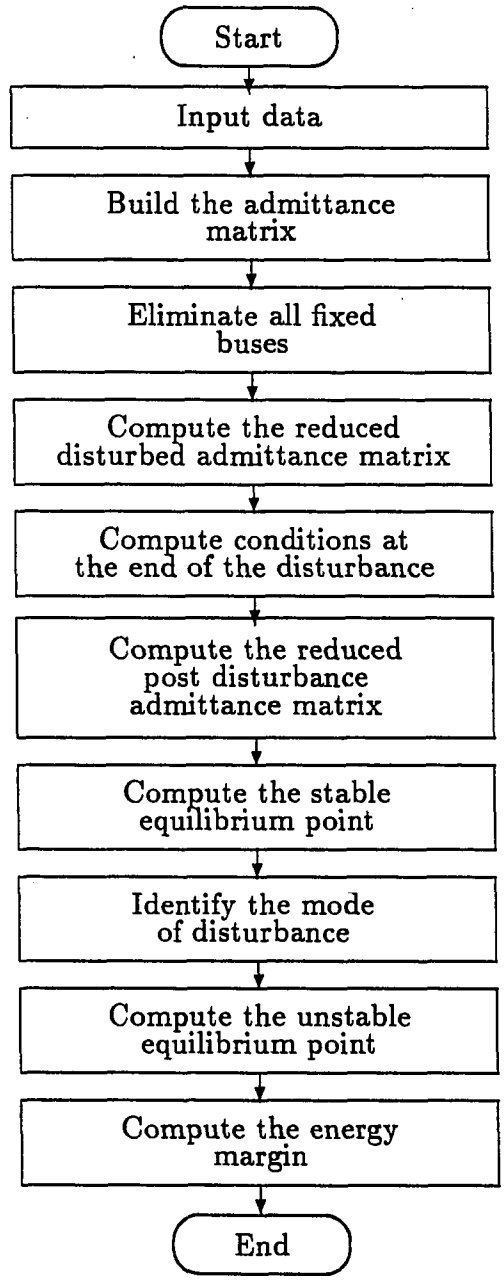

Figure 3.1: Flow Chart of the TEF Procedure

3.2 SEP and UEP Solution

In obtaining the SEP and UEP solution for the classical power system model in the center of inertia (COI) reference frame, the same set of nonlinear algebraic equations for the post disturbance network as in Chapter 2 are used. The starting point for the solution process is different for each case.

In obtaining the post disturbance $\mathbf{Y}_{BUS}$ matrix reduced to the internal generator nodes, the following steps are used, and the intermediate stages of the $\mathbf{Y}_{BUS}$ reduction saved to incorporate the nonlinear loads in the SEP and UEP solution.

1. Using the network admittance matrix including all load buses and generator terminal buses, and incorporating $1/jx'_d$ terms on the diagonal entries of the generator terminal buses, we obtain,

$$\begin{bmatrix} \underline{I}_1^A \\ \underline{I}_2^A \end{bmatrix} = \begin{bmatrix} \mathbf{Y}_{11}^A & \mathbf{Y}_{12}^A \\ \mathbf{Y}_{21}^A & \mathbf{Y}_{22}^A \end{bmatrix} \begin{bmatrix} \underline{V}_L \\ \underline{V}_G \end{bmatrix}$$

   The admittance matrix above is termed as $\mathbf{Y}_{BUS}^A$.

2. The above matrix is augmented with the internal generator buses and all the terminal buses are reduced to obtain,

$$\begin{bmatrix} \underline{I}_1^B \\ \underline{I}_2^B \end{bmatrix} = \begin{bmatrix} \mathbf{Y}_{11}^B & \mathbf{Y}_{12}^B \\ \mathbf{Y}_{21}^B & \mathbf{Y}_{22}^B \end{bmatrix} \begin{bmatrix} \underline{V}_L \\ \underline{E} \end{bmatrix}$$

   The above admittance matrix is termed as $\mathbf{Y}_{BUS}^B$. We retain the terminal buses of those generators at which loads are to be modeled.

3. Finally, all the load buses are reduced to obtain the admittance matrix reduced

to the internal nodes,

$$\left[\underline{I}_C \right] = \left[\mathbf{Y}_{BUS}^C \right] \left[\underline{E} \right]$$

These steps require no additional computation and are obtained as intermediate steps in the final reduction.

3.2.1 Procedure

1. At each load bus, the component of constant impedance load is folded into the $\mathbf{Y}_{BUS}$. For the constant current and constant MVA portions, evaluate current components,

$$\underline{I}_{CI}^0 = \left[\frac{[P_L^0 p_2 + jQ_L^0 q_2]}{V_L^0} \right]^*$$

$$\underline{I}_{CM}^0 = \left[\frac{[P_L^0 p_3 + jQ_L^0 q_3]}{V_L^0} \right]^* \qquad (3.1)$$

where,

P_L^0 - Pre-disturbance MW load

Q_L^0 - Pre-disturbance MVAR load

V_L^0 - Pre-disturbance load bus voltage

p_2, q_2 - multipliers for constant current MW and MVAR load components respectively

p_3, q_3 - multipliers for constant MVA, MW and MVAR load components respectively

2. Form $\underline{I}_{CI} + \underline{I}_{CM} = \underline{I}_1$.

   Using a source transformation evaluate the current injected (Norton equivalent source current) at the generator buses as $\underline{I}_2 = \frac{\underline{E}\angle\theta}{jx'_d}$

3. Solve for $\begin{bmatrix} \underline{V}_L \\ \underline{V}_G \end{bmatrix}$, using,

$$\begin{bmatrix} -\underline{I}_1 \\ \underline{I}_2 \end{bmatrix} = \begin{bmatrix} \mathbf{Y}^A_{BUS} \end{bmatrix} \begin{bmatrix} \underline{V}_L \\ \underline{V}_G \end{bmatrix} \tag{3.2}$$

   where $\mathbf{Y}^A_{BUS}$ is the network admittance matrix, which includes all the load buses and generator terminal buses, and incorporates $1/jx'_d$ on the diagonal entries of the generator terminal buses.

   Then update

$$\begin{aligned} \underline{I}_{CI} &= \left[\frac{P^0_L p_2 \frac{|V^{new}_L|}{|V^0_L|} + jQ^0_L q_2 \frac{|V^{new}_L|}{|V^0_L|}}{V^{new}_L} \right]^* \\ \underline{I}_{CM} &= \left[\frac{P^0_L p_3 + jQ^0_L q_3}{V^{new}_L} \right]^* \end{aligned} \tag{3.3}$$

   iterate over equations (3.2) and (3.3) until the difference in the magnitude of the current vector between successive iterations satisfies a given tolerance. In this research work, the iterative algorithm presented in [33] is used. A brief outline of the procedure is presented in the Appendix.

4. Using $\mathbf{Y}^B_{BUS}$, (which is the network admittance matrix corresponding to the load buses and generator internal buses) the current vector $\begin{bmatrix} -\underline{I}_1 \end{bmatrix}$ is reflected

onto the generator internal buses using the distribution factor approach suggested in [34]. After eliminating V_L, we write

$$\underline{I}_2 = -\mathbf{Y}_{21}^B \left[\mathbf{Y}_{11}^B\right]^{-1} \underline{I}_1 + \left[\mathbf{Y}_{22}^B - \mathbf{Y}_{21}^B \left[\mathbf{Y}_{11}^B\right]^{-1} \mathbf{Y}_{12}^B\right] \underline{E}_g$$

where

$$\underline{I}_{GL} = \left[\mathbf{Y}_{21}^B \left[\mathbf{Y}_{11}^B \right]^{-1} \right] \left[-\underline{I}_1 \right] \tag{3.4}$$

is the reflected current vector on the generator internal nodes.

5. Augment the electrical power output of each generator with a component corresponding to $\underline{I}_{GL}$,

$$P'_{ei} = P_{ei} + E_i I_{GL_i} cos(\theta_i - \phi_i) \tag{3.5}$$

where $I_{GL_i} \angle \phi_i$ is the complex reflected current.

6. Perform one iteration of the SEP and UEP solution using

$$P_i - P'_{ei} - \frac{M_i}{M_T} P'_{COI} = 0 \quad , i = 1, 2, \ldots, n \tag{3.6}$$

where

$$P'_{COI} = \sum_{i=1}^{n} (P_i - P'_{ei})$$

. Update the θ vector and evaluate the mismatches. If the solution converges stop, or else go to step 2.

3.3 Conditions at Fault Clearing

The conditions at fault clearing are determined using the approximate technique developed in [18]. In this technique, the acceleration is held constant over

each time step of the faulted period. The accelerating power for each machine is evaluated using a procedure identical to the SEP and UEP solution, where the component of current corresponding to the nonlinear loads is reflected onto the generator internal buses, at the beginning of each time step. The procedure for reflecting the currents is done using the faulted $\mathbf{Y}_{BUS}$ parameters. The time period from the instant of the fault t_0 to the instant of fault clearing t_f is divided into several intervals, each of length Δt. This technique is detailed below:

1. From the network solution of the faulted network, find the accelerating power as follows:

   - Apply steps 1 through 5 of the procedure detailed in section 3.2.1, using the faulted $\mathbf{Y}_{BUS}$ parameters, to get the augmented electrical power output of each generator $P_e(t_0)$, which includes the effects of the nonlinear loads.
   - Compute the accelerating power (during the fault) by:

$$P_a = P_e(t_{0-}) - P_e(t_{0+})$$

2. The speed change at the end of the first interval is given by

$$\Delta\omega(t_1) = \frac{P_a \Delta t}{2H} pu$$

3. The angle change is given by

$$\Delta\delta(t_1) = (2\pi f \times 180/\pi)\frac{P_a(\Delta t)^2}{4H} \; degrees$$

   and

$$\delta(t_1) = \delta(t_0) + \Delta\delta(t_1)$$

4. A new network solution is evaluated for the new position of the generator rotors and a new accelerating power $\tilde{P}_a$ is calculated using the same method as in step 1.

5. The parameters at the end of the susequent time intervals are

$$\Delta\omega(t) = \left(\Delta\omega(t_1) + \frac{\tilde{P}_a \Delta t}{2H}\right) pu$$

$$\Delta\delta(t) = (2\pi f \times 180/\pi)\left(\Delta\omega(t_1) \times \Delta t + \frac{\tilde{P}_a(\Delta t)^2}{4H}\right) degrees$$

3.4 Mode of Disturbance Evaluation

The MOD is evaluated using the ray point for each candidate mode [24]. The ray point is determined from the SEP, which incorporates the effect of the nonlinear loads. The procedure for determining the ray point is described below:
The UEPs of interest lie in the proximity of the corner points of a polytope [1]. For a given mode, e.g., determined by machines i and j having advanced angles, the corner point for an n-machine system would be $[\theta_1^s, \theta_2^s, \ldots, (\pi - \theta_i^s), \ldots, (\pi - \theta_j^s), \ldots, \theta_n^s]$. In angular space, a ray from $\underline{\theta}^s$ to the corrected corner point (which is the corner point corrected for the motion of the inertial center [23]) is formed. Along this ray, the potential energy is maximized, using a simple one dimensional maximization.

The rationale behind this procedure is that in the direction of the approximation to the UEP, we determine a point $\underline{\theta}^{ray}$ in angular space at which the potential energy is a maximum. This point resides on the PEBS, which is a surface connecting the various UEPs. Hence, a point on the PEBS offers a more realistic estimate of the UEP.

In order to evaluate the normalized potential energy margin to determine the MOD, the conditions at fault clearing are determined as described in section (3.3). It should be noted that during the motion along the ray the current injections have to be updated in order to evaluate the augmented electrical power. The steps involved in determining the energy margin are described in the following section.

3.5 Energy Margin Computation

Incorporating the component corresponding to the nonlinear loads, the expression for the system energy is given by

$$\begin{aligned} V &= \int \sum_{i=1}^{n} [M_i \dot{\tilde{\omega}}_i - P_i + P_{ei} + E_i I_{GL_i} cos(\theta_i - \phi_i) \\ &\quad + \frac{M_i}{M_T} P'_{COI}] \dot{\theta}_i dt \end{aligned} \tag{3.7}$$

where $\tilde{\omega}_i$ is the rotor speed with respect to the COI. Integrating the above expressions between suitable limits, the expression for the transient energy function, based on the linear trajectory approximation [18] for the transfer conductance terms, is given by,

$$\begin{aligned} V &= \frac{1}{2} \sum_{i=1}^{n} M_i \tilde{\omega}_i^2 - \sum_{i=1}^{n} P_i(\theta_i - \theta_i^s) - \sum_{i=1}^{n-1} \sum_{j=i+1}^{n} [C_{ij}(cos\theta_{ij} - cos\theta_{ij}^s) \\ &\quad - \frac{(\theta_i + \theta_j - \theta_i^s - \theta_j^s)}{(\theta_{ij} - \theta_{ij}^s)} D_{ij}(sin\theta_{ij} - sin\theta_{ij}^s)] \\ &\quad + \sum_{i=1}^{n} \int_{\theta_i^s}^{\theta_i} E_i I_{GL_i} cos(\theta_i - \phi_i) d\theta_i \end{aligned} \tag{3.8}$$

The expression for the energy margin using the corrected kinetic energy [18] is

then given by

$$\begin{aligned}\Delta V &= -\frac{1}{2}\sum_{i=1}^{n} M_i \tilde{\omega}_{eq}^{cl\,2} - \sum_{i=1}^{n} P_i(\theta_i^u - \theta_i^{cl}) - \sum_{i=1}^{n-1}\sum_{j=i+1}^{n} [C_{ij}(cos\theta_{ij}^u - cos\theta_{ij}^{cl}) \\ &\quad - \frac{(\theta_i^u + \theta_j^u - \theta_i^{cl} - \theta_j^{cl})}{(\theta_{ij}^u - \theta_{ij}^{cl})} D_{ij}(sin\theta_{ij}^u - sin\theta_{ij}^{cl})] \\ &\quad + \sum_{i=1}^{n} \int_{\theta_i^{cl}}^{\theta_i^u} E_i I_{GL_i} cos(\theta_i - \phi_i) d\theta_i \end{aligned} \tag{3.9}$$

where

M_{eq} - $\frac{M_{cr} M_{sys}}{M_T}$

$\tilde{\omega}_{eq}^{cl}$ - $\tilde{\omega}_{cr}^{cl} - \tilde{\omega}_{sys}^{cl}$

θ^u - rotor angles at the controlling UEP

θ^{cl} - rotor angles at fault clearing

M_{cr} - sum of inertias of machines included in the MOD of the controlling UEP

M_{sys} - sum of inertias of the remainder of the machines

$\tilde{\omega}_{cr}^{cl}$ - inertial center speed at fault clearing of machines included in the MOD of the controlling UEP

$\tilde{\omega}_{sys}^{cl}$ - inertial center speed at fault clearing of the remaining machines

The last term in equation (3.9) is path dependent and is evaluated by assuming a linear trajectory between $\underline{\theta}^{cl}$ and $\underline{\theta}^u$. This trajectory is divided into several parts. Numerical verification of this division on several systems has shown that the value

of the expression remains essentially unchanged when the number of divisions is increased beyond ten. Thus, we have,

$$\theta_i^k = \theta_i^{cl} + \frac{k}{10}(\theta_i^u - \theta_i^{cl}) \quad , k = 0, 1, 2, \ldots, 10 \tag{3.10}$$

At each point on the linear trajectory (i.e., for $k = 0, \ldots, 10$), knowing the vector $\underline{\theta}$, obtain the injected currents at the generator buses and the network bus voltages, using the procedure detailed in Section (3.2). Now, update the load currents to maintain their nonlinear characteristics and compute the reflected current vector $\underline{I}_{GL}$ using equation (3.4). Using trapezoidal integration the energy component is computed and the energy margin is obtained.

4 NUMERICAL RESULTS FOR NONLINEAR LOADS

4.1 Test Systems

The technique proposed in Chapter 3 was verified on two test systems: a 4-generator test system and a 17-generator equivalent of the network of the State of Iowa.

4.1.1 4-generator Test System

This test system of 4 generators and 11 buses shown in Figure 4.1 is a modified version of the 9-bus, 3-machine, 3-load system widely used in the literature and often referred to as the WSCC test system. This system is described in detail in reference [18]. The generator data and the initial operating conditions are given in Table 4.1. This system was investigated for a three phase fault on bus #10 cleared by opening one of the lines between bus 10-8.

4.1.2 17-generator Test System

This test system of 17 generators and 162 buses is a reduced Iowa system model obtained from the power network of the state of Iowa. This system is also described in detail in reference [18]. The generator data and the system operating conditions are given in Table 4.2 and the network is shown in Figure 4.2. Three disturbances

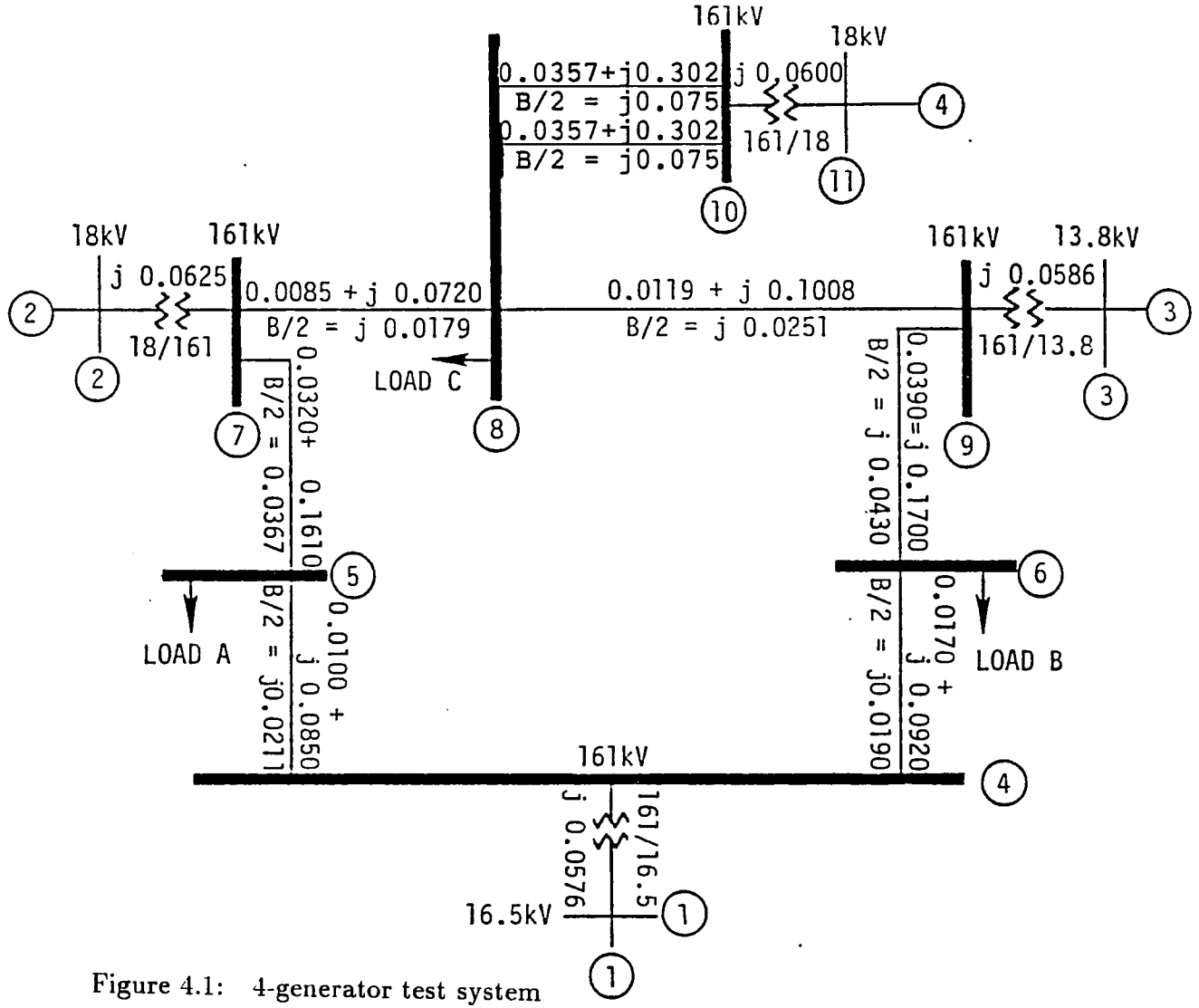

Figure 4.1: 4-generator test system

Table 4.1: Generator data and initial conditions of the 4-generator system

Generator	Generator Parameters			Initial Conditions Internal Voltage	
Number	H (MW/MVA)	x'_d (pu)	P_{mo}[a] (pu)	E (pu)	δ (degree)
1	23.64	0.0608	2.269	1.0967	6.95
2	6.40	0.1198	1.600	1.1019	13.49
3	3.01	0.1813	1.000	1.1125	8.21
4	6.40	0.1198	1.600	1.0741	24.90

[a] On a 100-MVA base.

Table 4.2: Generator data and initial conditions of the 17-generator system

Generator Number	Generator Parameters			Initial Conditions Internal Voltage	
	H (MW/MVA)	x'_d (pu)	P_{mo}[a] (pu)	E (pu)	δ (degree)
1	100.00	0.0040	20.000	1.00319	-27.93
2	34.56	0.0437	7.940	1.13339	-1.34
3	80.00	0.0100	15.000	1.03015	-16.32
4	80.00	0.0050	15.000	1.00112	-26.10
5	16.79	0.0507	4.470	1.06797	-6.23
6	32.49	0.0206	10.550	1.05056	-4.57
7	6.65	0.1131	1.309	1.01611	-23.04
8	2.66	0.3115	.820	1.12349	-26.95
9	29.60	0.0535	5.519	1.11932	-12.40
10	5.00	0.1770	1.310	1.06521	-11.12
11	11.31	0.1049	1.730	1.07776	-24.35
12	19.79	0.0297	6.200	1.06094	-10.12
13	200.00	0.0020	25.709	1.01058	-28.15
14	200.00	0.0020	23.875	1.02059	-26.73
15	100.00	0.0040	24.670	1.01861	-21.10
16	28.60	0.0559	4.550	1.12434	-6.68
17	20.66	0.0544	5.750	1.11168	-4.40

[a] On a 100-MVA base.

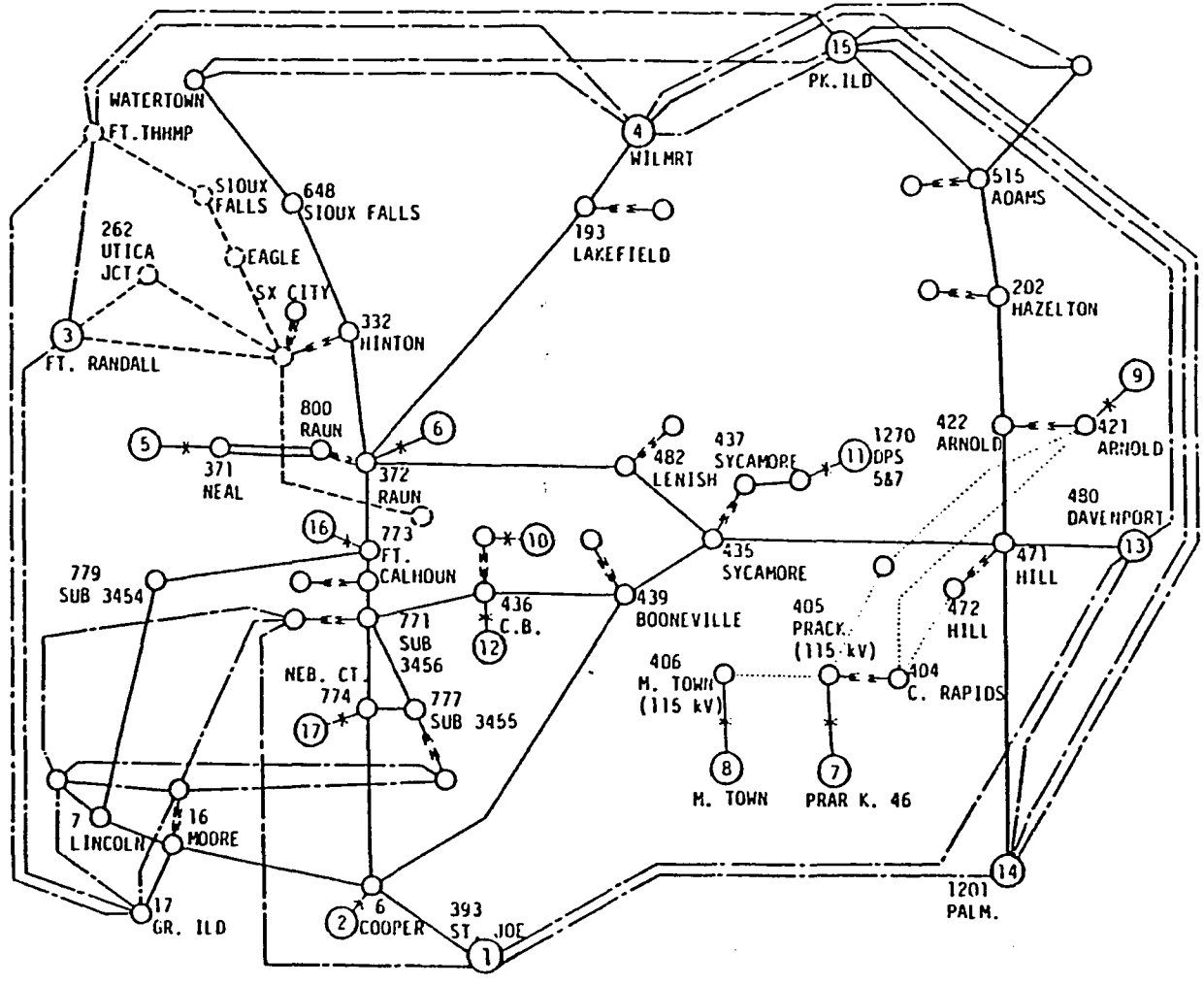

Figure 4.2: 17-generator test system

were investigated for this system:

1. A three phase fault at Council Bluffs (C.B.) unit no. 3 (bus #436), cleared by opening line 436-771.

2. A three phase fault at Cooper (bus #6), cleared by opening line 6-774.

3. A three phase fault at Fort Calhoun (bus #773), cleared by opening line 773-779.

In all the cases, the critical clearing time was used as a measure of transient stability assessment. The results obtained using the TEF method were compared with time simulation results using the EPRI-745 program.

4.2 Numerical Results

The results for the 4-generator system are shown in Table 4.3. Three different combinations of nonlinear loads are considered. Since the TEF method has been well established using constant impedance loads, only combinations of constant current and constant MVA loads have been considered here.

The results in Table 4.3 show that the proposed procedure provides an accurate assessment of transient stability in terms of clearing times. The normalized energy margin ΔV_n, in the TEF also gives an estimate of the degree of stability (or instability). The proposed technique reliably brackets the clearing times for the stable and unstable cases and provides good comparison with time simulation results.

Table 4.4 shows the results for the 17-generator system. In this system, for all the three fault locations considered, the load composition is 100% constant current.

Table 4.3: Stability assessment for 4-generator system

Case No.	Load Composition	Time Simulation		TEF Method			
		Critically Stable Case	Critically Unstable Case	Critically Stable Case		Critically Unstable Case	
		t^{cl}s	t^{cl}s	t^{cl}s	ΔV_n pu	t^{cl}s	ΔV_n pu
1	100% Const. I	0.12	0.125	0.10	0.399	0.12	-0.023
2	80% Const. I 20% Const. MVA	0.105	0.11	0.105	0.081	0.11	-0.0129
3	60% Const. I 40% Const. MVA	0.10	0.105	0.10	0.0013	0.105	-0.0878

Table 4.4: Stability assessment for 17-generator system

Case No.	Load Composition	Time Simulation		TEF Method			
		Critically Stable Case	Critically Unstable Case	Critically Stable Case		Critically Unstable Case	
		t^{cl}s	t^{cl}s	t^{cl}s	ΔV_n pu	t^{cl}s	ΔV_n pu
1	100% Const. I	0.18	0.20	0.18	0.1787	0.20	-0.2995
2	100% Const. I	0.20	0.21	0.19	0.1143	0.20	-0.1408
3	100% Const. I	0.31	0.32	0.33	0.0685	0.35	-0.2106

Table 4.5: Results for 17-generator system with 100% constant impedance loads

Case No.	Load Composition	Time Simulation		TEF Method	
		Critically Stable Case	Critically Unstable Case	Critically Stable Case	Critically Unstable Case
		t^{cl}s	t^{cl}s	t^{cl}s	t^{cl}s
1	100% Const. Z	0.20	0.204	0.20	0.204
2	100% Const. Z	0.204	0.212	0.204	0.212
3	100% Const. Z	0.345	0.357	0.345	0.356

Table 4.5 shows the results for 100% constant impedance loads. Comparing the critical clearing times obtained for the constant current load representation and the constant impedance load representation, we see that the critical clearing times for the constant current load representation are smaller than those for the constant impedance load representation. Thus, we see a definite need to model nonlinear loads in power systems stability analysis.

The results presented in Table 4.4 again indicate that the proposed technique provides stability assessment, which compares fairly accurately with the time simulation results.

5 APPLICATIONS OF THE TEF METHOD TO STRESSED LARGE-SCALE POWER SYSTEMS

5.1 Need for Analysis of Stressed Large Scale Power Systems

The advent of extensive interconnected operation in North America and the inability of utilities to install additional transmission capacity has led to the maximum loading of transmission lines in certain regions.

In many parts of the network, the stressed conditions are created by:

- a high level of system loading,
- heavy power transfers across certain transmission interfaces, and
- heavy loading of certain plants for economic operation.

Under these stressed conditions the power system is vulnerable to disturbances that can affect reliability.

When the area of system stress encompasses most of the interconnected system, the system has to be represented in its entirety. In such cases, geographically remote disturbances can have an effect upon the other portions of the system.

Moreover, it may be necessary to identify exactly the key areas that separate from the system in extreme situations. Hence, it is necessary to represent the stressed systems in large scale for stability studies.

5.2 Difference in Analysis Between Unstressed and Stressed Systems

The most common applications of the TEF method involve moderately loaded power system, which is brought to instability by an increased disturbance magnitude (e.g., longer fault duration). Most of these applications are limited to demonstrating the usefulness of the method in small or medium size power systems. The critical clearing times of disturbances are used as the basis for comparing the results of the TEF method to those obtained by conventional means. The transient behavior of system in these cases is easy to predict and the behavior is dominated by the effect of fault location and duration. The limiting conditions of interest (e.g., power flows) are usually limited by the duration of the fault and perhaps by the power generation of units close to the location of the fault.

In contrast, a stressed system may exhibit a complex dynamic behavior. As indicated before, stressed conditions arise due to increased power transfers and heavy loading of transmission systems. In such a situation, when a large disturbance of short duration occurs, the disturbance may be cleared by losing a key transmission facility. In some extreme situations of transmission inadequacies, the post disturbance system may not even be steady-state stable. A typical stability study of interest in the operation of the stressed systems is arriving at the transient stability limits in terms of critical transmission interface power flow limits and critical plant generation limits. Such a study is aimed at computing the guidelines for operating limits of certain power flows or generation, constrained by the stability of the system.

The post disturbance network of the stressed system is characterized by weak synchronizing forces caused by large transmission impedances. The generators away

from the fault location may also separate from the system.

5.3 Inter-Area Mode

The dynamic phenomenon can be described as follows: Following the disturbance, a small group of generators close to the fault location are severely disturbed initially. But, as the transient progresses, the weak synchronizing forces in the system dominate. When instability occurs, it takes place as a separation of a large group of generators (including the small group severely disturbed by the fault initially) from the rest of the system. This is the so-called "inter-area" mode phenomenon of stressed systems. In extreme situations of instability, the post disturbance network, with loss of critical transmission facility, may not even be steady-state stable. The stability limited conditions of interest in operating the stressed systems (e.g., power transfer across a critical transmission interface) may be limited by the power generation levels of units far away from the fault location.

The analysis of transients in a stressed system can therefore be complex. When first swing transient analysis is made by conventional means, the time solution must be run for a period of 2-3 seconds to detect the system separation and the areas that separate. The analysis of inter-area mode phenomenon by the direct method based on TEF method, can also be a complex task. A host of analytical and numerical issues are encountered and must be dealt with.

The accurate assessment of the critical energy depends primarily on the determination of MOD, therefore it is crucial to select the candidate modes properly in order to determine the actual MOD. The number of generators can be very large in the stressed large-scale system. Hence, the selection of candidate modes by the

analyst is virtually impossible. Thus, it is vital to develop the TEF method to accommodate the automatic selection of candidate modes.

5.4 MOD Shift

The scheme for determining the MOD in the present version of the TEF program, accurately predicts the mode of disturbance in the UEP of interest in case of unstressed systems. The mode of disturbance selected by this scheme in the stressed cases usually consists of machines which are electrically close to the disturbance location and severely disturbed initially. The UEP solution obtained using the MOD selected, however, contains many more advanced generators, indicating the existence of the inter-area mode of system separation.

Thus, the MOD predicted in these cases is invariably a small group of generators that are severely affected initially and the true mode of disturbance is a large group of generators splitting from the system due to dominance of inter-area mode over the initial disturbance.

Consider the following example [23]: In the Ontario-Hydro 50-generator system with Nanticoke generation at 3700 MW, a three-phase fault on the Nanticoke 500 KV bus, cleared by opening Nanticoke-Milton 500 KV line at 0.108 secs, the MOD (predicted) comprises of two Nanticoke generators. The starting point (ray point) has these two machines advanced. However, the Corrected Gauss Newton (CGN) method of solution, when started with this point, converges to a UEP with 29 machines advanced, which includes the two generators of the predicted MOD. In this case the two Bruce machines were heavily loaded with 3160 MW, and the transmission system has limitations caused by losing a 500 KV line.

Thus, the initially predicted MOD is different from the final MOD, in this case. Presently in the TEF method there is a UEP verification scheme which verifies the MOD shift [23]. However, this verification scheme is only "after the fact" and what we need is a technique which would predict the onset of the inter-area mode. We will see how this is done in the following sections.

5.5 Identification of Inter-Area Mode possibility

As seen from the preceding section, in some cases, the final MOD is different from the initially predicted MOD. Hence, we need some technique which would identify the inter-area mode possibility. The technique suggested in this research to identify the inter-area mode possibility is based on the theory of modal analysis.

5.5.1 System Equations

We write equation (2.5) in the state space form as:

$$\begin{bmatrix} \dot{\underline{\theta}} \\ \dot{\underline{\tilde{\omega}}} \end{bmatrix} = \begin{bmatrix} \mathbf{O} & \mathbf{I} \\ \mathbf{M}^{-1}\mathbf{J} & \mathbf{O} \end{bmatrix} \begin{bmatrix} \underline{\theta} \\ \underline{\tilde{\omega}} \end{bmatrix} \tag{5.1}$$

where, $\mathbf{J} = \left[\frac{\partial f_i}{\partial \theta_j}\right]$ $, i,j = 1,2,\ldots,(n_g - 1)$ *with* n_g = *no of generators*, is the Jacobian matrix evaluated at the post disturbance SEP and $\underline{\theta}$ *and* $\underline{\tilde{\omega}}$ are vectors of perturbations in machine angles and speeds (in COI reference) respectively. This is of the form

$$\dot{\underline{X}} = \mathbf{A}\underline{X} \tag{5.2}$$

where, $\mathbf{A}$ is the $n \times n$ (where $n = 2(n_g - 1)$) plant matrix and is given by

$$\mathbf{A} = \begin{bmatrix} \mathbf{O} & \mathbf{I} \\ \mathbf{M}^{-1}\mathbf{J} & \mathbf{O} \end{bmatrix} \tag{5.3}$$

and $\underline{X}(t)$ is a $n \times 1$ state vector whose variation with time defines the free motion of the system.

5.5.2 Free Response Characteristics

The precise nature of the free motion of the above continuous time system following any disturbance can be described very simply in terms of the eigenvalues and eigenvectors of the plant matrix $\mathbf{A}$ [35,36]. The eigenvectors of the system in equation (5.1) are easily shown to be the square roots of the eigenvalues of $\mathbf{M}^{-1}\mathbf{J}$ [36]. The system in equation (5.1) in fact has purely imaginary eigenvalues (occurring in conjugate pairs), which are distinct [36]. It is well-known [35] that if $\mathbf{A}$ has n distinct eigenvalues λ_i(i=1,2,...,n), then it will also have n corresponding linearly independent $n \times 1$ eigenvectors $\underline{u}_i (i = 1, 2, \ldots, n)$ which are related by the equations

$$\mathbf{A}\underline{u}_i = \lambda_i \underline{u}_i \quad i = 1, 2, \ldots, n \tag{5.4}$$

In addition to the eigen properties of $\mathbf{A}$, the corresponding properties of the transposed matrix $\mathbf{A}'$, play an important role in the modal analysis of the system. Also, $\mathbf{A}$ and $\mathbf{A}'$ have the same eigenvalues [35]. The $n \times 1$ eigenvectors $\underline{v}_j (j = 1, 2, \ldots, n)$ of $\mathbf{A}'$ are related by the equations

$$\mathbf{A}'\underline{v}_j = \lambda_j \underline{v}_j \quad j = 1, 2, \ldots, n$$

or

$$\underline{v}_j'\mathbf{A} = \lambda_j\underline{v}_j' \quad j = 1,2,\ldots,n \tag{5.5}$$

It is convenient to normalize the eigenvectors $\underline{u}_i$ and $\underline{v}_j$. Let $\mathbf{U} = [\underline{u}_1, \underline{u}_2, \ldots, \underline{u}_n]$ be the $n \times n$ modal matrix of $\mathbf{A}$ and $\mathbf{V} = [\underline{v}_1, \underline{v}_2, \ldots, \underline{v}_n]$ be the $n \times n$ modal matrix of $\mathbf{A}'$. Let $\mathbf{\Lambda} = diag[\lambda_1, \lambda_2, \ldots, \lambda_n]$. Then we have the following [35]

$$\mathbf{AU} = \mathbf{U\Lambda} \tag{5.6}$$

$$\mathbf{A'V} = \mathbf{V\Lambda} \tag{5.7}$$

$$\mathbf{V'U} = \mathbf{I}_n \tag{5.8}$$

Now, introduce a new state vector $\underline{\xi}(t)$, by the following transformation

$$\underline{X}(t) = \mathbf{U}\underline{\xi}(t) \tag{5.9}$$

Then we have from equation (5.2),

$$\mathbf{U}\dot{\underline{\xi}}(t) = \mathbf{AU}\underline{\xi}(t) \tag{5.10}$$

$$\dot{\underline{\xi}}(t) = \mathbf{U}^{-1}\mathbf{AU}\underline{\xi}(t) \tag{5.11}$$

$$\dot{\underline{\xi}}(t) = \mathbf{\Lambda}\underline{\xi}(t) \tag{5.12}$$

The importance of equation (5.12) as compared with equation (5.2) is that $\mathbf{\Lambda}$ is a diagonal matrix, whereas $\mathbf{A}$ is, in general, non-diagonal.

Equation (5.12) clearly implies that

$$\dot{\xi}_i(t) = \lambda_i\xi_i(t) \quad i = 1,2,\ldots,n \tag{5.13}$$

and the solution of these equations are given by the formulae

$$\xi_i(t) = \xi_i(0)e^{\lambda_i t} \quad i = 1,2,\ldots,n \tag{5.14}$$

Therefore, $\underline{X}(t)$ is given by

$$\underline{X}(t) = \mathbf{U}\underline{\xi}(t) = [\underline{u}_1, \underline{u}_2, \ldots, \underline{u}_n] \begin{bmatrix} \xi_1(t) \\ \xi_2(t) \\ \vdots \\ \xi_n(t) \end{bmatrix} \tag{5.15}$$

$$\underline{X}(t) = \underline{u}_1\xi_1(0)e^{\lambda 1 t} + \underline{u}_2\xi_2(0)e^{\lambda 2 t} + \cdots + \underline{u}_n\xi_n(0)e^{\lambda n t} \tag{5.16}$$

Putting $t = 0$, we get

$$\underline{X}(0) = \underline{u}_1\xi_1(0) + \underline{u}_2\xi_2(0) + \cdots + \underline{u}_n\xi_n(0) \tag{5.17}$$

From equation (5.8) we get

$$\xi_i(0) = \underline{v}_i'\underline{X}(0) \tag{5.18}$$

(5.19)

From equations (5.16) we have,

$$\underline{X}(t) = \underline{u}_1\underline{v}_1'\underline{X}(0)e^{\lambda 1 t} + \underline{u}_2\underline{v}_2'\underline{X}(0)e^{\lambda 2 t} + \cdots + \underline{u}_n\underline{v}_n'\underline{X}(0)e^{\lambda n t} \tag{5.20}$$

or

$$\underline{X}(t) = \sum_{i=1}^{n} e^{\lambda_i t}\underline{u}_i\underline{v}_i'\underline{X}(0) \tag{5.21}$$

This equation clearly shows that the free motion of the continuous time system governed by equation (5.2) is a linear combination of n functions of the form $e^{\lambda_i t}\underline{u}_i$ $(i = 1, 2, \ldots, n)$ which are said to describe the n dynamical modes of the system. Thus the "shape" of a mode is described by its associated eigenvector $\underline{u}_i$, and its time domain characteristics by its associated eigenvalue λ_i.

5.5.3 Participation Factors

It has often been suggested that the significant state variables in each mode are those that correspond to large entries in the eigenvector $\underline{u}_i$, where $\underline{u}_i$ is the right eigenvector associated with eigenvalue λ_i and is given by equation (5.4). An obvious objection to this, is that the entries of $\underline{u}_i$ are, in general, incommensurable (for example, $\underline{u}_i$ consists of machine angles and speeds) and that changing the units in which the state variables are measured will correspondingly change the magnitudes of the entries of $\underline{u}_i$, except for those entries that happen to be zero to begin with [36].

A related, but dimensionless measure of state variable participation (or participation of machines) in a mode i may be obtained by examining not only the right eigenvectors $\underline{u}_i$ but also the associated left eigenvectors $\underline{v}_i'$ defined via equations (5.5). While the right eigenvector gives the "mode shape" (by describing the activity of the variables when the mode is excited), the left eigenvector gives the "mode composition", which describes what weighted combination of state variables is needed to construct the mode (see equations (5.17) and (5.18)). Mathematically, this can be seen by noting that the variable associated with the i^{th} mode is obtained by "diagonalizing" equation (5.2). We can write

$$\underline{\xi}(t) = \mathbf{U}^{-1}\underline{X}(t) \tag{5.22}$$

Thus, from equation (5.8) we have

$$\underline{\xi}(t) = \mathbf{V}'\underline{X}(t) \tag{5.23}$$

or

$$\xi_i(t) = \underline{v}_i'\underline{X}(t) \quad i = 1, 2, \ldots, n$$

(5.24)

Thus, from equations (5.21) and (5.8) we have

$$\begin{aligned} \xi_i(t) &= \underline{v}_i' e^{\lambda_i t} \underline{u}_i \underline{v}_i' \underline{X}(0) \\ &= \underline{v}_i' \underline{X}(0) e^{\lambda_i t} \sum_{k=1}^{n} v_{ki} u_{ki} \end{aligned} \tag{5.25}$$

where v_{ki} and u_{ki} denote the k^{th} component of the eigenvectors $\underline{v}_i$ and $\underline{u}_i$, respectively. The above equation suggests that the participation of the k^{th} state variable $\underline{X}_k$ in the i^{th} mode may be measured via its "participation factor" [36],

$$p_{ki} = v_{ki} u_{ki} \tag{5.26}$$

This quantity is dimensionless and is therefore not affected by change of scale on the variables. Thus, we may think of u_{ki} as measuring the activity of $\underline{X}_k$ in the i^{th} mode and v_{ki} as weighting the contribution of this activity to the mode. (It may also be noted that, $p_{ki} = \frac{\partial \lambda_i}{\partial a_{kk}}$, where a_{kk} is the diagonal entry of the plant matrix **A**, is in fact the eigenvalue sensitivity, which relates changes in λ_i to changes in a_{kk}.)

5.5.4 Excitation of the Modes

Let

$$\begin{aligned} \alpha_i &= \underline{v}_i' \underline{X}(0) \quad , i = 1, 2, \ldots, n \\ &= \xi_i(0) \end{aligned} \tag{5.27}$$

Then, equation (5.21) can be written as [37]

$$\underline{X}(t) = \sum_{i=1}^{n} \alpha_i e^{\lambda_i t} \underline{u}_i \tag{5.28}$$

Now, we say that only one mode of oscillation, or briefly one mode, in particular the i^{th} mode of the realization is excited, if

$$\underline{X}(t) = e^{\lambda_i t}\underline{c} \tag{5.29}$$

where $\underline{c}$ is a constant vector proportional to the eigenvector $\underline{u}_i$.

The significant thing is that every component of $\underline{X}$ varies with time in the same way, namely as $e^{\lambda_i t}$. The modes have several important properties [37]:

1. There are n modes, one for each eigenvalue λ_i.

2. Each mode is excited independently of the other modes, i.e., an arbitrary initial condition will, in general, excite all the modes, but the amount, $\alpha_i = \underline{v}_i' \underline{X}(0)$, of excitation, is clearly independent of that of any other mode.

3. The excitation of each mode depends only on the initial state [38].

Equation (5.28) is a linear combination of the n functions of the form $e^{\lambda_i t}\underline{u}_i$, $i = 1, 2, \ldots, n$, (which are said to describe the n dynamical modes of the system) each weighted by α_i. This equation is the same as equation (5.21), where the "shape" of a mode was described by its associated right eigenvector $\underline{u}_i$ and its time domain characteristic by its associated eigenvalue λ_i. Also, it has been shown that eigenvalues and eigenvectors provide a profound insight into the system behavior [39] and that this insight can further be improved by the introduction of "dominance measures", which are the weights α_i in equation (5.28). By the aid of these dominance measures, the dominant modes (or eigenvalues) can be chosen. It should be noted that the dominant modes selected in this way need not have the largest eigenvector norms. As indicated earlier, the entries in the eigenvector

$\underline{u}_i$ are, in general, incommensurable, as they consist of machine angles and speeds, and hence, we cannot pick large entries in the eigenvector as the significant state variables. Thus, we measure the participation of a state variable in a chosen mode via its participation factors as explained earlier in section 5.5.3. Also, we use the dominance measure, α_i, to give an indication of the dominant modes. The procedure for selecting the dominant modes is described in the next section. Thus, α_i can give an indication of the dominant modes. Computing the participation factors for each of the dominant modes will give us the participation of the various state variables (see equation (5.25)) in these modes.

5.6 Procedure

From the above observations, we can arrive at an algorithm to select the dominant modes by examining both the magnitudes and angles of the $\alpha_i's$. This is demonstrated in the section on selection of modes.

5.6.1 Eigenvalues and Eigenvectors of A

- Run the TEF program to get the Jacobian **J** at the post disturbance SEP. This is done in order to represent the dynamic behavior of the power system for perturbations around the nominal operating condition of interest, which is the post disturbance condition. The aim is to study the stability behavior of the post disturbance system. Hence, linearization of the equations around the post disturbance SEP could result in a better approximation of the trajectory behavior.

- Form the plant matrix **A** using equation (5.3).
- Compute the eigenvalues ($\lambda_i,\ i = 1,2,\ldots,n$), right eigenvectors ($\underline{u}_i, i = 1,2,\ldots,n$) and left eigenvectors ($\underline{v}_i, i = 1,2,\ldots,n$) of **A**.
- Select initial value of $\underline{X}$, i.e., $\underline{X}(0)$ based on the angles and speeds at clearing as

$$\underline{X}(0) = \begin{bmatrix} \theta_1^{cl} - \theta_1^s \\ \theta_2^{cl} - \theta_2^s \\ \vdots \\ \theta_{ng-1}^{cl} - \theta_{ng-1}^s \\ \tilde{\omega}_1^{cl} \\ \tilde{\omega}_2^{cl} \\ \vdots \\ \tilde{\omega}_{ng-1}^{cl} \end{bmatrix} \tag{5.30}$$

where θ_i^{cl} and θ_i^s are the clearing angle and SEP angle of the i^{th} machine respectively, in COI reference and $\tilde{\omega}_i^{cl}$ is the clearing speed of the i^{th} machine in COI reference.

5.6.2 Selection of Modes

In this section we will use the "dominance measure" to select the dominant modes. As indicated earlier, the α_i's are weights in equation (5.28) and to select the dominant mode we could just select the α_i which is the largest. However, α_i is a complex number, which has a magnitude and an angle. Thus, we need to collect α's with similar angles, and then we can simply compare their magnitudes and pick the

one with the largest magnitude. Also, since the angles of α's lie in a wide range, we need to group them in various groups with similar angles, so that we can compare magnitudes of those with similar angles. This grouping is of significance in that it gives us some idea of the modes which interact. This interaction of modes will be further enhanced by the inclusion of the second order terms, as will be explained in section 5.7.

Thus, the procedure for selecting the modes is as follows:

- Compute α_i , $i = 1, 2, \ldots, n$ using equation (5.27). (It should be remembered that α is a complex number.)
- Group modes which have angles of α within $20^\circ - 30^\circ$. This will give us several groups.
- Within each group, order the modes with decreasing magnitude of α.
- Choose the first few modes from each group (for instance, those with magnitude of α upto 10-15% of the magnitude of the largest α).
- Compute the participation factors for the chosen modes using $p_{ki} = v_{ki} u_{ki}, k = 1, 2, \ldots, n,\ i \in I$ where I is the set containing the chosen modes.
- Examine the participation factors $p_{ki}, k = 1, 2, \ldots, n$ for each mode $i \in I$.
- Pick the states k which give a significant value of p_{ki} (for instance, $p_{ki} \geq 0.1$) for each mode $i \in I$.
- These states k correspond to the machine (angles and speeds), which participate in the i^{th} mode. We make a table for each $i \in I$ and machines participating in that mode.

- In these tables if the machines picked up by the MOD test appear in just one mode, or appear in a mode just by themselves, then we have a simple mode. The MOD test in the TEF method is based on the lowest normalized potential energy margin as detailed in [23]. The MOD is a terminology for characterizing the controlling UEP, in which the angles of a certain group of generators are advanced (generally, greater than $\pi/2$ radians).

- If the machines picked up by the MOD test appear in more than one mode, or in different modes, then we have a superposition of modes. In other words, if these machines participate in more than one mode then there is an indication of the interaction of these modes which could result in an inter-area mode or a complex mode.

5.7 Inclusion of Second Order Terms

The method of analysis used in section (5.5) is to linearize the differential equations describing the system behavior (equation (2.5)) by assuming small changes in the system quantities or the state variables. Equations for these variables are then found by making a Taylor series expansion around the post disturbance SEP and neglecting the higher order terms. Equation (5.1) results from the Taylor series expansion upto the first order terms. In stressed systems, the expansion of the nonlinear equations upto the first order terms may not be sufficient to understand the system behavior. Hence, we need to include some of the higher order terms (for e.g., the second order terms) also. Thus, we approximate equation(2.5) after

including the second order terms as follows:

$$\begin{aligned} \dot{\underline{\theta}}_i &= \underline{\omega}_i \\ \dot{\underline{\omega}}_i &= \frac{\mathbf{J}_i}{M_i}\underline{\theta} + \frac{1}{2M_i}\underline{\theta}^T \mathbf{G}^i \underline{\theta} \quad i = 1, 2, \ldots, n_g - 1 \end{aligned} \tag{5.31}$$

where

$\mathbf{J}_i = i^{th}$ row of Jacobian

$\mathbf{G}^i$=Hessian matrix for $f_i = \left[\frac{\partial^2 f_i}{\partial\theta_j \partial\theta_k}\right]$ $, j, k = 1, 2, \ldots, (n_g - 1)$

The expression for $\mathbf{G}^i$ is given in [23]. Writing this in the form of equation (5.2), we have:

$$\dot{X}_i = \mathbf{A}_i \underline{X} + \frac{1}{2}\underline{X}^T \mathbf{H}^i \underline{X} \quad i = 1, 2, \ldots, n \tag{5.32}$$

where $\mathbf{A}_i$ $= i^{th}$ row of the plant matrix $\mathbf{A}$

$$\mathbf{H}^i = \begin{bmatrix} \mathbf{O} & \mathbf{O} \\ \mathbf{O} & \mathbf{O} \end{bmatrix} \text{ for } i = 1, 2, \ldots, n_g - 1$$

$$\mathbf{H}^i = \begin{bmatrix} \mathbf{O} & \mathbf{O} \\ \frac{\mathbf{G}^{i-(n_g-1)}}{M_{i-(n_g-1)}} & \mathbf{O} \end{bmatrix} \text{ for } i = n_g, \ldots, n$$

where $\mathbf{O}$ is the null matrix of order $(n_g - 1)$.

Again, we apply the transformation

$$\underline{X}(t) = \mathbf{U}\underline{\xi}(t)$$

With this transformation, we can analyze equation (5.32) in terms of the modes, rather than the states. Equation (5.32) then takes the form

$$\begin{aligned}\dot{\xi}_m &= \lambda_m \xi_m + \frac{1}{2}\sum_{p=1}^{n}\xi_p^2 \sum_{q=1}^{n} u_{qp} \sum_{k=1}^{n}\sum_{i=1}^{n} v_{km} H_{iq}^k u_{ip} \\ &+\frac{1}{2}\sum_{p=1}^{n-1}\sum_{q=p+1}^{n}\xi_p\xi_q[u_{pq}\sum_{k=1}^{n}\sum_{i=1}^{n} v_{km}H_{ip}^k u_{ip} + u_{pp}\sum_{k=1}^{n}\sum_{i=1}^{n} v_{km}H_{ip}^k u_{iq} \\ &+u_{qp}\sum_{k=1}^{n}\sum_{i=1}^{n} v_{km}H_{iq}^k u_{iq} + u_{qq}\sum_{k=1}^{n}\sum_{i=1}^{n} v_{km}H_{iq}^k u_{ip} \\ &+\sum_{\substack{r=1\\ r\neq p,q}}^{n} u_{rq}\sum_{k=1}^{n}\sum_{i=1}^{n} v_{km}H_{ir}^k u_{ip} + u_{rp}\sum_{k=1}^{n}\sum_{i=1}^{n} v_{km}H_{ir}^k u_{iq}] \\ &, m = 1,2,\ldots,n \end{aligned} \tag{5.33}$$

where $\mathbf{U} = [u_{pq}]$, $p,q = 1,2,\ldots,n$ is the modal matrix described earlier and $\mathbf{V} = [v_{pq}]$, $p,q = 1,2,\ldots,n$ is the inverse of $\mathbf{U}$. From this equation, we see that

$$\begin{aligned}\dot{\xi}_m &= c_{0m}\xi_m + \sum_{p=1}^{n} c_{1mp}\xi_p^2 + \sum_{p=1}^{n-1}\sum_{q=p+1}^{n} c_{2mpq}\xi_p\xi_q \\ &, m = 1,2,\ldots,n \end{aligned} \tag{5.34}$$

The effect of the inclusion of the higher order terms can be observed by examining equation (5.34). Note that $c_{0m} = \lambda_m$ and this represents the free response. The coefficients c_{1mp} and c_{2mpq} represent the interaction of the various modes. Based on the magnitude of c_{1mp}, the effect of the various modes ξ_p on ξ_m can be determined. In addition, the magnitude of c_{2mpq} will determine the extent of the interaction of the modes p and q.

The procedure can be described as follows:

- Select a mode m from those selected by considering only the first order terms.
- Compute the coefficients c_{0m}, c_{1mp} and c_{2mpq} for this mode.

- Compare the magnitudes of the coefficients c_{1mp} and c_{2mpq} with that of c_{0m}.
- List the p or p *and* q for those coefficients which are significant in magnitude when compared to c_{0m}.
- Modes p and p *and* q seem to interact with mode m.

The results for the inclusion of the second order terms are discussed in the next chapter.

6 NUMERICAL RESULTS FOR THE INTER-AREA MODE PHENOMENON

6.1 Test Systems

The technique proposed in Chapter 5 was verified on three test systems: a 17-generator equivalent of the network of the state of Iowa, the 50-generator Ontario Hydro system and the 126-generator dynamic equivalent of the western USA system.

6.1.1 17-Generator Test System

This test system is the same as that used in Chapter 4. The area of interest is in the western part of the network (along the Missouri river), where several generating plants are located. A disturbance in this part of the network substantially influences the motion of several generators. Thus, very complex modes of instability can occur (and have been encountered in earlier research projects), offering a severe test to the procedure developed in Chapter 5.

The inter-area mode investigation was conducted for the Cooper case and the Fort Calhoun case. The Cooper case represents a system with a simple mode, whereas the Fort Calhoun case exhibits a complex mode.

6.1.2 50-Generator Test System

This test system comprises of 50 generators and 196 buses of the Nanticoke subsystem of the Ontario Hydro interconnected grid. The critical generators of the Nanticoke and Bruce complex of this system are shown in Figure 6.1. In this investigation, the "unstressed situation" can be typically referred to a condition when the Bruce (nuclear) units are not heavily loaded (Bruce generation is about 1400 MW and Nanticoke generation is about 3840 MW). The "stressed situation", on the other hand, represents the condition of heavy generation schedule at Bruce units (Bruce generation is increased to about 3160 MW, with Nanticoke generation at 3900 MW), causing the transmission lines in this part of the network to be heavily loaded. The disturbance which is introduced close to the Nanticoke complex, is a fault at the Nanticoke bus, cleared by opening a 500 kv transmission line. The stability limits of interest in this case are the generation at the Bruce and Nanticoke complex.

6.1.3 126-Generator Test System

This test system is a dynamic equivalent of the western USA system obtained from Salt River Project, Phoenix, Arizona [40]. This equivalent consists of 1443 buses, 2215 branches and 126 machines. Figure 6.2 gives a schematic arrangement of the generators in the system. Each box in this figure represents an area and each number in the box represents a generator. The arrows between the boxes indicate the direction of the prefault power flows. For the case under study, the total generation in the system is 68968 MW. For this particular distribution of generation, the transmission network is heavily loaded which leads to a highly stressed system.

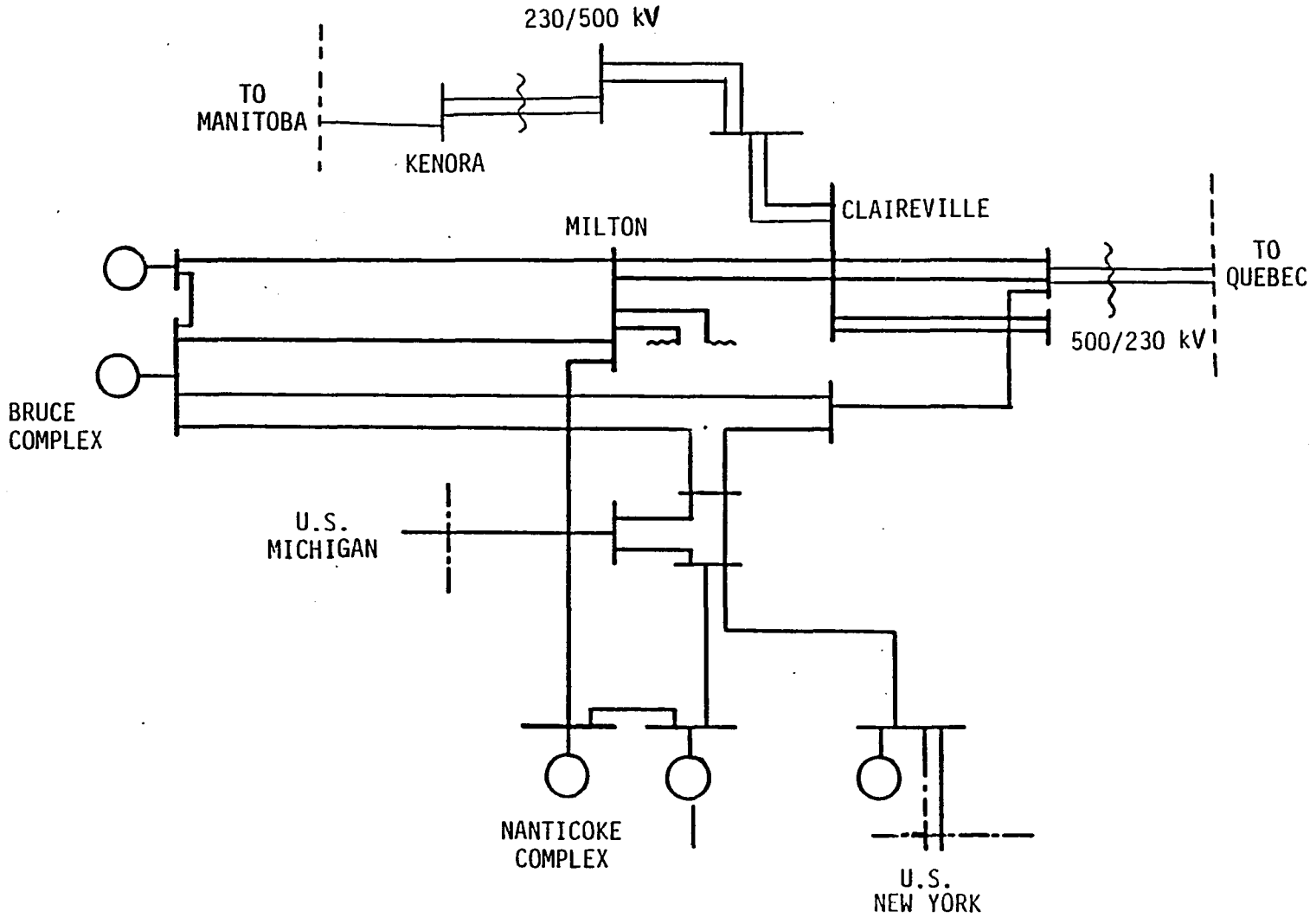

Figure 6.1: Portion of the Ontario Hydro system showing the critical generators

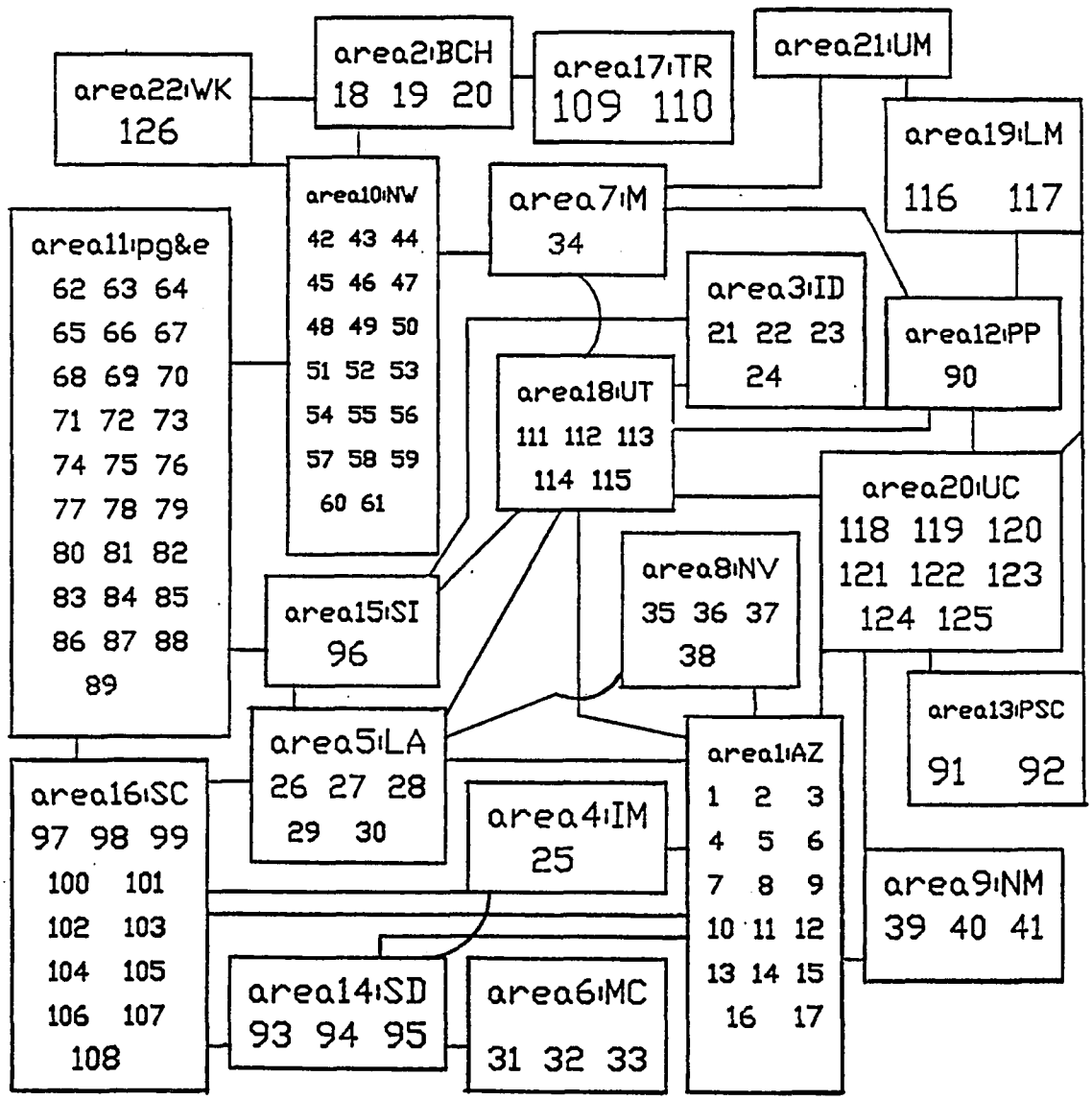

Figure 6.2: Schematic arrangement for generators in SRP system

One sign of the high degree of stress in the system is large machine angles at the prefault SEP for machines in Areas 2, 17 and 22. The largest machine in the system (both in inertia and mechanical power) is machine #13 (Palo Verde) in area 1 (Arizona). Another characteristic feature of this system is that there are three large machines (equivalents) close to each other in area 2 (B.C.Hydro). This group, which consists of machines #18, 19 and 20 exports power to the southern part of the system.

The fault considered is a 3-phase fault applied on the 500 KV side of machine #13's step up transformer and is cleared by removing the 500 KV line between Palo Verde and Devers.

6.2 Numerical Results with First Order Terms

6.2.1 17-generator system

The following indicates the application of the technique presented in Chapter 5 to the 17-generator system with the same loading, but for faults at different locations. The following results demonstrate how the fault location affects the selection of the modes.

6.2.1.1 Simple MOD Table 6.1 depicts the grouping of the α's for the various modes for the 17-generator system (Cooper case). The MOD test (presently available in the TEF program) picks machine #2. This machine appears only in mode #13 in Table 6.1. This appears to be a simple MOD, since the machine picked by the MOD test in the TEF method appears only in one mode. From the table, we see that for mode #13 the magnitude of α is 4.2035 and the eigenvector norm is

Table 6.1: 17-Generator System (Cooper Fault)

Group	Mode	Alpha		Eigenvector Norm	Machines picked by Participation Factor
		Magnitude	Angle		
1	13	4.2035	-44.92	0.94787	2
	19	2.0508	-36.65	0.73465	17
2	3	1.3530	120.58	0.47591	1
3	15	0.6637	-29.63	0.98095	11
	17	0.2762	-18.87	0.69658	5,6
4	25	0.0297	-102.37	0.94229	7

Table 6.2: 17-Generator System Participation Factors (Cooper Fault)

Mode	Participating Machines (Participation Factors)
13	2(0.2941)
19	17(0.3032)
3	1(0.1685)
15	11(0.4101)
17	5(0.1841), 6(0.1431)
25	7(0.3988)

0.94787. This eigenvector norm is not the largest. As indicated earlier, the selection of modes is not based on the largest eigenvector norm alone, but is based on the groupings according to the angle of α's and the magnitudes of the α's. Examining the participation factors for mode #13, from Table 6.2, we see that machine #2 has the largest participation factor of 0.2941, and hence, we pick machine #2 as participating in mode #13. The time domain simulation confirms this MOD [18].

6.2.1.2 Complex MOD Table 6.3 shows the grouping of the α's for the 17-generator Fort Calhoun case. The MOD test in the TEF method picks up machines #2, 5, 6, 10, 12, 16 and 17 as the advanced machines. From Table 6.3 we

Table 6.3: 17-Generator System (Ft. Calhoun Fault)

Group	Mode	Alpha		Eigenvector Norm	Machines picked by Participation Factor
		Magnitude	Angle		
1	11	4.0303	148.32	0.92539	16
	5	1.4376	141.63	0.75070	3
2	25	2.6756	-19.25	0.79731	17
	3	1.9917	-40.74	0.44868	1
	27	1.3745	-18.11	0.87255	2,1
3	21	1.6079	160.95	1.12276	10,17
	31	1.1699	175.88	0.73034	5,6
4	13	1.0612	71.24	8.98735	12

can see that the machines picked up by the MOD test in the TEF method appear in different selected modes, for e.g., mode #11 picks machine #16, mode #25 picks machine #17, mode #27 picks machine #2, mode #21 picks machine #10 and 17, mode #31 picks machines #5 and 6 and mode #13 picks machine #12. Table 6.4 shows the participating machines with their participation factors for all the selected modes. Since the machines picked up by the MOD test in the TEF method appear in different selected modes, we see an interaction of modes #11,25,27,21,31 and 13, which gives rise to a complex mode. The time domain simulation also confirms the above machines as going unstable [18]. The results of Table 6.3 indicate a superposition of modes or an inter-area phenomenon. All the machines picked up by the MOD test are being picked up by this technique. Another point to note is that machines #1 and 3 can be eliminated from the table, as they are not advanced in the post disturbance period, since their angles at clearing are less than their SEP angles.

Table 6.4: 17-Generator System Participation Factors (Ft. Calhoun Fault)

Mode	Participating Machines (Participation Factors)
11	16(0.2470)
5	3(0.3082)
25	17(0.3056)
3	1(0.1619)
27	2(0.2823), 1(0.1683)
21	10(0.3506), 17(0.1019)
31	5(0.1812), 6(0.1398)
13	12(0.2730)

6.2.2 50-generator system

The following indicates the application of the technique of Chapter 5 to a system with the same fault clearing times, but with different loading conditions as described in Section 5.1.2. The following results demonstrate how the system loading affects the interaction of the various modes and hence their selection.

6.2.2.1 Simple MOD Table 6.5 shows the grouping of the α's for the various modes for the 50-generator unstressed system. In this case, the MOD test in the TEF method, picks up machines #20 and 26. From Table 6.5, we can see that machines #20 and 26 appear independently only in mode #31. Here again, this appears to be a simple MOD, since the machines picked up by the MOD test in the TEF method, appear only in one mode. Looking at the participation factors, from Table 6.6, for mode #31, we see that machines #20 and 26 have the largest participation factors (0.3087 and 0.1866 respectively).

Table 6.5: 50-Generator System (Unstressed Case)

Group	Mode	Alpha		Eigenvector Norm	Machines picked by Participation Factor
		Magnitude	Angle		
1	91	1.6933	-80.29	6.38624	7
	93	1.4065	-80.99	4.81269	41
2	87	1.3469	92.26	2.00828	7,41
3	31	0.9801	-75.75	0.86132	20,26
	65	0.7926	-67.49	1.00298	12
4	55	0.7898	113.97	0.93566	39
	67	0.7804	114.99	2.01499	12
5	19	0.4729	-142.59	13.16788	13
6	37	0.4025	77.48	0.87778	43
7	1	0.3204	-22.56	0.91988	2,35
8	13	0.2374	142.12	0.76119	3
9	75	0.1522	-133.09	0.53933	21
10	57	0.0939	121.65	1.96810	39,5
11	53	0.0353	24.05	0.60087	46

Table 6.6: 50-Generator System Participation Factors (Unstressed Case)

Mode	Participating Machines (Participation Factors)
91	7(0.1612)
93	41(0.1126)
87	7((0.1806), 41(0.1760)
31	20(0.3087), 26(0.1866)
65	12(0.1704)
55	39(0.1358)
67	12(0.3183)
19	13(0.3683)
37	43(0.3567)
1	2(0.3849),35(0.1122)
13	3((0.4207)
75	21(0.1074)
57	39(0.1841),5(0.1276)
53	46(0.1514)

Table 6.7: 50-Generator System (Stressed Case)

Group	Mode	Alpha		Eigenvector	Machines picked by
		Magnitude	Angle	Norm	Participation Factor
1	89	2.8562	-76.73	2.83310	2,18,20,etc.
	31	1.1003	-67.85	0.72014	20,26,27
	33	1.0002	-77.53	1.09871	27
	67	0.9888	-68.05	1.06567	12
	69	0.8768	-66.59	1.69417	12
	21	0.6382	-52.49	1.01244	13
	17	0.1368	-40.40	0.80277	14,16
2	87	2.8179	104.57	5.36859	41
	57	1.1744	115.09	0.94930	5,39
	85	0.4602	103.41	0.89355	48
3	79	1.4184	-83.55	1.74620	7
	39	0.90728	-95.70	0.95425	43
	81	0.2355	-86.26	0.69677	9,25
	61	0.1319	-87.23	1.20443	4
4	77	1.2795	88.46	0.87458	26
	37	0.8796	82.10	0.47105	2,6,20,etc.
	49	0.5795	86.92	1.07466	10
	55	0.3502	79.13	0.42536	25
	41	0.2996	91.24	0.45985	45
	23	0.1437	98.71	1.01275	8
5	25	0.5411	125.49	1.02674	34
	9	0.2007	132.92	0.82326	23
	19	0.0625	127.77	0.89195	24
6	1	0.5265	-19.35	0.91910	2,35
	13	0.1549	-34.05	0.78735	3
7	11	0.1626	-171.62	0.96250	17
	65	0.0892	-144.59	0.80315	19,16
	95	0.0268	-164.33	9.55355	49
8	5	0.09815	147.29	0.87599	30,31
	75	0.0948	150.79	0.61764	46
9	53	0.0298	168.88	0.42895	46
	3	0.0168	164.77	0.99417	1
10	97	0.0197	40.01	0.88220	22,21

Table 6.8: 50-Generator System Participation Factors (Stressed Case)

Mode	Participating Machines (Participation Factors)
89	2(0.0129), 18(0.0102), 20(0.0309), etc.
31	20(0.2291), 26(0.1617), 27(0.1024)
33	27(0.3514)
67	12(0.3834)
69	12(0.1032)
21	13(0.3896)
17	16(0.2816), 14(0.1900)
87	41(0.1907)
57	5(0.1573), 39(0.1132)
85	48(0.1015)
79	7(0.3421)
39	43(0.4380)
81	9(0.2813), 25(0.1603)
61	4(0.4043)
77	26(0.1062)
37	2(0.0109), 6(0.0115), 20(0.0160), etc.
49	10(0.2697)
55	25(0.1337)
41	45(0.1063)
23	8(0.4382)
25	34(0.3229)
9	23(0.3805)
19	24(0.3622)
1	2(0.3836), 35(0.1135)
13	3(0.4281)
11	17(0.4467)
65	19(0.2089), 16(0.1025)
95	49(0.4740)
5	30(0.3451), 31(0.1382)
75	46(0.1246)
53	46(0.1289)
3	1(0.4583)
97	22(0.3356), 21(0.1581)

6.2.2.2 Complex MOD For the 50-generator stressed case, the MOD test in the TEF method, again picks machines #20 and 26. The mode in which machines #20 and 26 appear by themselves in the simple MOD case, disappears and mode #31 now picks machines #20,26 and 27. We see from Table 6.7 that the machines #20 and 26 appear in mode #31 and that machine #26 also appears in mode #77 by itself. Thus, we see an interaction of modes #31 and 77. Table 6.8 shows the participating machines with their participation factors for all the selected modes. Since, the machines picked up by the MOD test in the TEF method, appear in different selected modes, we see a superposition of modes and conclude that this case exhibits a complex mode. It should be noted that the exact UEP for this case and the time domain simulation pick up the 28 machines: #1, 2, 3, 4, 5, 6, 7, 8, 9, 10, 11 ,12, 13, 14, 15, 16, 17, 19, 20, 21, 22, 23, 24, 25, 26, 27, 34, and 35. as advanced and most of these machines are being picked up by this test. In an earlier research work [41], the thinking was that in the stressed case the 2-machine mode shifts to the 28-machine mode, but the results of this research work seem to indicate that there is no mode which picks all these machines, instead several modes interact with each other and result in the inter-area mode phenomenon.

6.2.3 126-generator SRP system

This system has been studied in detail in reference [40]. The behavior of the system is such that for a clearing time of 15 cycles, it is the machine closest to the fault, machine #13 that goes unstable, but when the fault duration is decreased, a larger group of machines goes unstable. The time domain simulation results clearly indicate this [40].

The following indicates the application of the technique in Chapter 5 to a system with the same loading, but with different fault clearing times. The following results demonstrate how the fault clearing time affects the selection of the modes. It should be noted that $\underline{X}(0)$ depends on the angles and speeds at clearing. The following results also indicate the effect of fault clearing time on the interaction of the various modes.

6.2.3.1 Simple MOD For the 15 cycles clearing case, Table 6.9 shows the groupings of the α's for the various modes. The MOD test in the TEF method, picks up machine #13 (Palo Verde). Machine #13 appears all by itself only in one of the selected modes (in mode #17). Table 6.10 shows the participating machines along with their participation factors for all the selected modes. It should be noted that although machine #13 is picked up in modes #23 and 43, along with other machines, it has a participation factor (0.0669 and 0.0458 respectively) which is not very significant when compared with the participation factor (0.1205) when it appears all by itself in mode #17. From the table we can see that the magnitude of α for mode #17 is 0.8125 and the eigenvector norm is 0.18732. Looking at the participation factors for mode #17, we pick machine #13 which has the largest participation factor of 0.1205. This appears to be a simple MOD, since the machine picked up by the MOD test in the TEF method, appears significantly only in one mode.

Table 6.9: 126-Generator System (15 cycles clearing)

Group	Mode	Alpha		Eigenvector Norm	Machines picked by Participation Factor
		Magnitude	Angle		
1	81	5.3390	-51.08	1.01882	39
	179	1.9638	-43.16	0.85080	93,108
2	137	4.5982	132.85	1.08985	49,58
	43	2.2805	121.68	0.46059	13,21,66, etc.
3	101	2.9795	150.02	0.96922	17
	121	0.6503	160.68	0.73410	6
4	23	1.8131	-63.45	0.25372	8,13,21, etc.
	13	0.6712	-87.31	0.21972	18,19,20
5	33	0.8787	-4.86	0.97452	25
	111	0.5462	-27.6	0.58799	31,33
6	17	0.8125	105.23	0.18732	13
	203	0.4202	114.65	0.93583	14
7	45	0.3705	3.24	0.66484	4,123
	109	0.3379	21.02	0.66413	12
8	53	0.1586	-172.89	0.61415	7,40
	27	0.0548	-178.84	0.93128	113,114
9	129	0.1363	68.05	9.84153	76
10	133	0.1192	55.99	0.89579	97
11	1	0.0984	-101.88	0.99991	111
	7	0.0116	-91.94	0.82370	81,82
12	39	0.0089	-125.91	0.91970	63

Table 6.10: 126-Generator System Participation Factors (15 cycles clearing)

Mode	Participating Machines (Participation Factors)
81	39(0.1926)
179	93(0.2124), 108(0.1103)
137	49(0.2416), 58(0.1752)
43	13(0.0459), 21(0.0312), 66(0.0169), etc.
101	17(0.4216)
121	6(0.2732)
23	8(0.0106), 13(0.0669), 21(0.0117), etc.
13	18(0.1428), 19(0.1442), 20(0.1355)
33	25(0.4673)
111	31(0.1540), 33(0.1965)
17	13(0.1205)
203	14(0.3196)
45	4(0.1277), 123(0.1512)
109	12(0.3081)
53	7(0.1939), 40(0.1295)
27	113(0.1322),114(0.3036)
129	76(0.4104)
133	97(0.3771)
1	111(0.4985)
7	81(0.1304), 82(0.3607)
39	63(0.4222)

6.2.3.2 Complex MOD For the 8.5 cycles clearing case, Table 6.11 shows the grouping of the α's for the various modes. The machine picked up by the MOD test in the TEF method, is machine #13 and this appears in several of the selected modes (#23,43 and 63). Machine #13 does not appear all by itself in any of the modes, i.e., the mode in which machine #13 appears by itself, disappears. Table 6.12 shows the participating machines with their participation factors for all the selected modes. In all the selected modes, machine #13 does not have a participation factor ≥ 0.1. For selected modes #23,43 and 63, the participation factor of all machines is small and machine #13 does have a significant participation factor compared to the other machines. Also, from the time domain simulation [40], we see that machine #18,19,20,44,109,110 and 126 are the ones that go unstable. These machines appear in different selected modes, for e.g., machines #18,19 and 20 appear in mode #13, machine #44 in mode #173, machines #109 and 110 in mode #113 and machine #126 in mode #249. Thus, all the machines which go unstable (from the time domain simulation) are being picked up by this technique. The machine picked up by the MOD test in the TEF method, appears in different selected modes, thus indicating a superposition of modes or a complex MOD.

Table 6.11: 126-Generator System (8.5 cycles clearing)

Group	Mode	Alpha		Eigenvector Norm	Machines picked by Participation Factor
		Magnitude	Angle		
1	81	2.4991	-70.45	1.01852	39
	23	0.9572	-82.17	0.25372	8,13,21 etc.
2	137	2.1668	115.07	1.08985	15
	43	1.1568	101.43	0.46059	13,21,66, etc.
	63	0.92731	108.47	0.36756	10,13,22, etc.
3	101	1.4769	131.05	0.96922	17
	121	0.4114	135.48	0.73410	6
4	117	0.7559	-50.37	0.99389	1
	33	0.6316	-30.77	0.77452	25
5	13	0.3695	-97.28	0.21972	18,19,20
	141	0.0546	-91.58	0.90964	96
6	1	0.1235	167.73	0.99991	111
	217	0.0583	169.75	0.83516	104
7	5	0.1191	38.95	14.2025	65
	203	0.0891	55.33	0.93583	14
8	133	0.0945	-22.99	0.89579	97
	249	0.0017	-14.15	1.33727	126
9	197	0.0344	-140.65	1.13434	100,105
	163	0.0062	-134.82	0.62270	22
10	157	0.0151	70.15	0.83259	107
	113	0.0003	84.14	0.84458	109,110
11	173	0.0011	-166.08	0.84082	44

Table 6.12: 126-Generator System Participation Factors (8.5 cycles clearing)

Mode	Participating Machines (Participation Factors)
81	39(0.1926)
23	8(0.0106), 13(0.0669), 21(0.0117), etc.
137	15(0.4777)
43	13(0.0459), 21(0.0312), 66(0.0169), etc.
63	10(0.0468), 13(0.0479), 27(0.0866), etc.
101	17(0.4216)
121	6(0.2731)
117	1(0.3726)
33	25(0.4673)
13	18(0.1428), 19(0.1443), 20(0.1355)
141	96(0.3338)
1	111(0.4985)
217	104(0.3328)
5	65(0.4988)
203	14(0.3195)
133	97(0.3770)
249	126(0.4132)
197	100(0.1653), 105(0.2049)
163	22(0.1968)
157	107(0.3311)
113	109(0.1292), 110(0.3439)
173	44(0.4025)

6.3 Numerical Results of Inclusion of Second Order Terms

6.3.1 17-generator system Ft. Calhoun case

Table 6.13 lists the coefficients c_{0m}, c_{1mp} and c_{2mpq} for the various modes which were selected in Table 6.3. From Table 6.13, we see that for selected mode #11, the magnitude of coefficients c_{1mp} for p=3,25 are comparable with the magnitude of c_{0m}, which is, in fact λ_{11}. From equation (5.34), we see that c_{1mp},p=3,25 are coefficients (or weights) of the squared terms ξ_p^2,p=3,25. Thus, based on the theory developed in section (5.7), we conclude that modes #3 and 25 interact with mode #11, since their coefficients (or weights) are comparable with λ_{11}. Also, from Table 6.3, we see that modes #3 and 25 are amongst the selected modes, thus confirming the superposition or interaction of modes. From Table 6.13, for mode #11, the magnitude of c_{2mpq} for p=1 and q= 3 and 25 are also comparable with the magnitude of c_{0m} $(= \lambda_{11})$. From equation (5.34), we note that these coefficients, c_{2mpq}, are the coefficients (or weights) of the product terms $\xi_p \xi_q$. Again, we conclude that modes #1,3 and 25 interact with mode #11, thus confirming the superposition of modes. Similarly, modes #1,3, and 27 interact with mode #5 and modes #1,3,7,11,15,17,21 and 31 interact with mode #13.

The machines picked up by their participation factors in the various modes selected based on the first and second order terms are: # 2, 5, 6, 10, 12, 16 and 17.

6.3.2 50-generator system stressed case

Table 6.14 lists the coefficients c_{0m}, c_{1mp} and c_{2mpq} for the modes # 31,33,11 and 49, which were selected in Table 6.9. From the first group of entries in this

Table 6.13: 17-generator system coefficients for second order terms

Mode		Mode p coefficient		Mode p and q coefficient		
m	$\|c_{0m}\|$	p	$\|c_{1mp}\|$	p	q	$\|c_{2mpq}\|$
11	8.185	3	8.603	1	3	8.315
		25	9.322	1	25	8.288
5	6.838	3	11.883	1	3	8.853
				3	27	6.857
13	12.719	1	23.173	1	31	20.689
		3	19.126	3	31	14.153
		7	13.415	11	31	14.376
		17	17.511	15	21	12.707
		31	17.059			

table, we see that mode 31 interacts with modes 37,41,43,45,47,49 and 51. Most of these modes are being selected in Table 6.9 (i.e., by considering only the first order terms). The machines picked up by the various modes selected based on the first and second order terms are all the machines appearing in the UEP, except machine # 15. However, machine # 15 is located in the same plant as the Bruce machines # 9 and 25, thus it will be selected when the Bruce machines are chosen. Thus, the results of the inclusion of the second order terms indicate the interactions of the various modes and confirm the inter-area mode phenomenon or the complex MOD for the above cases.

Table 6.14: 50-generator system coefficients for second order terms

Mode		Mode p coefficient		Mode p and q coefficient		
m	$\lvert c_{0m}\rvert$	p	$\lvert c_{1mp}\rvert$	p	q	$\lvert c_{2mpq}\rvert$
31	11.138	43	12.659	37	41	16.298
				41	43	13.610
				43	45	18.546
				43	47	10.646
				43	49	12.917
				45	49	10.415
				49	51	10.997
33	11.086	31	9.391	5	35	9.329
		35	10.834	5	53	13.035
		37	13.045	15	35	12.068
		41	19.990	15	63	14.256
		43	10.500	23	41	16.385
		53	26.009	31	55	18.563
		55	11.782	31	77	15.344
		63	16.137	31	81	11.325
		75	22.936	35	63	24.992
		77	9.109	35	75	11.335
11	15.328			37	55	14.622
49	4.511	41	4.042	41	53	5.284
				43	53	5.687

7 CONCLUSIONS

Incorporation of the nonlinear load models in the TEF method involved the following four phases:

1. Accounting for the load behavior in the SEP and UEP solutions.
2. Determining the conditions at fault clearing and evaluating the MOD after incorporating the effects of the nonlinear loads.
3. Modifying the energy function to account for the nonlinear loads.
4. Validating and verifying the results of the nonlinear load incorporation.

The technique developed in Chapter 3 was tested on two test systems, which included the 4-generator WSCC system and the 17-generator reduced Iowa system. This technique was tested for different load compositions, different fault locations and different fault clearing times.

From the results presented in Chapter 4, the following conclusions can be drawn:

1. The proposed technique provides results which compare favorably with time simulation results.
2. The technique is generalized and can deal with any desired load composition.

The application of the modal analysis theory in identification of the inter-area mode possibility involved the following five phases:

1. Setting up the system equations for the free response characteristics.
2. Computation of the excitation or the "dominance measures" of the modes and thereafter selecting the dominant modes.
3. Applying the theory of including the second order terms to confirm the selection of modes picked up by the "dominance measures".
4. Comparing the results with those obtained by time domain simulations.
5. Indicating that the inter-area mode phenomenon, if present, results from the interaction among various modes.

The technique developed in Chapter 5 was tested on three test networks, which included the 17-generator reduced Iowa system, the 50-generator Ontario Hydro system and the 126-generator SRP system. This technique was tested for different fault configurations, different system loading conditions and different fault clearing times.

From the results presented in Chapter 6, the following conclusions can be drawn:

1. The theory of modal analysis can be applied to study the interaction of various modes and thus to indicate the inter-area mode possibility.
2. The technique accounts for the conditions at fault clearing through the initial vector $\underline{X}(0)$.

3. The technique accounts for the system configuration and loading via the post disturbance admittance matrices, which are used in computing the plant matrix **A**.

4. The technique gives a reasonably correct indication of the inter-area mode phenomenon by indicating the interactions of the various modes.

5. For the unstressed system (simple MOD cases), it is sufficient to consider the Taylor series expansion of the nonlinear equations upto the first order terms only.

6. For the stressed systems, where the system nonlinearity may become dominant, the second order terms in the series expansion for the state variables, also need to be considered.

7. Prelimnary results on the inclusion of the second order terms in the series expansion clearly indicate the interaction between the various modes, and detect the possibility of complex modes of oscillation.

8. The computational burden can be very heavy, when considering the second order terms, for a case with a large number of generators. In dealing with such situations some criteria to reduce the numerical burden need to be developed.

7.1 Suggestions for Future Research

Based on the experience of this research work, the following developments are recommended.

1. Load characteristics should be regarded as important as other system parameters, and every effort should be made to determine them in a realistic way. Most available test information on load characteristics is on the variation of active load with voltage [28]. There is somewhat less information on the variation of reactive load. When it comes to the effect of frequency, the test information is very scanty for active load, and practically nonexistent for reactive load. Thus, more attention should be devoted to analyzing the nature of the loads.

2. Sparse network formulation, preserving the network structure, may be attempted for incorporating the nonlinear load models.

3. Expansion of the nonlinear equations to include the higher order terms (as in Chapter 5) may be investigated further by applying it to the 126-generator system, in order to get additional information about the interaction of the various modes in stressed systems.

4. As mentioned before, the computational burden can be very heavy, when considering the second order terms, for a case with a large number of generators. To deal with such situations, it is proposed that the generators which are not of interest be eliminated, thus reducing the size and hence the computational burden. This proposal needs to be investigated and tested.

5. The inter-area mode of system separation is found to be a slowly developing transient. The effect of very fast exciters may be included to obtain more accurate computations of stability limits in the operation of stressed systems.

8 BIBLIOGRAPHY

[1] Pai, M. A. *Power System Stability Analysis by the Direct Method of Lyapunov.* North-Holland Systems and Control Series. Vol. 3. New York: North-Holland, 1981.

[2] "DIRECT - Fast Stability Program Using Direct Solution Techniques." EPRI Technical Brief, RP2206, Sheet No. 87, 1987.

[3] Kimbark, E. W. *Power System Stability.* Vol. I. New York: John Wiley & Sons, Inc., 1948.

[4] *Criteria of Stability of Electric Power Systems.* A report published by the all Union Institute of Scientific and Technological Information and the Academy of Sciences of the USSR Electric Technology and Electric Power Series, Moscow, USSR, 1971.

[5] Magnusson, P. C. "Transient Energy Method of Calculating Stability." *AIEE Trans.* 66 (1947): 747-755.

[6] Aylett, P. D. "The Energy Integral Criterion of Transient Stability Limits of Power Systems." *Proceedings of the IEE* 105(C) (1958): 527-536.

[7] Gless, G. E. "Direct Method of Lyapunov Applied to Transient Power System Stability." *IEEE Trans.* PAS-85 (February 1966): 159-168.

[8] El-Abiad, A. H. and K. Nagappan. "Transient Stability Regions of Multimachine Power Systems." *IEEE Trans.* PAS-85 (February 1966): 169-179.

[9] Gupta, C. L. and A. H. El-Abiad. "Determination of the Closest Unstable Equilibrium State for Lyapunov Methods in Transient Stability Studies." *IEEE Trans.* PAS-94 (September 1976): 1699-1712.

[10] Fouad, A. A. "Stability Theory - Criteria for Transient Stability." *Proc. Conference on Systems Engineering for Power: Status and Prospects,* Henniker, NH, 1975, Publication No. CONF-750867: 421-450.

[11] Ribbens-Pavella, M. "Transient Stability of Multimachine Power Systems by Lyapunov's Direct Method." *Proc. of Seminar on Stability of Large Scale Power Systems at University of Liege,* Liege, Belgium, 1972.

[12] Lugtu, R. L. and A. A. Fouad. "Transient Stability Analysis of Power Systems Using Lyapunov's Second Method." *IEEE Winter Meeting*, Paper No. C72145-6, New York, February 1972.

[13] Tavora, C. J. and Smith, D. J. M. "Characterization of Equilibrium and Stability in Power Systems." *IEEE Trans.* PAS-91 (May 1972): 1127-1130.

[14] Athay, T., R. Podmore and S. Virmani. "A Practical Method for Direct Analysis of Transient Stability." *IEEE Trans.* PAS-98 (1979): 573:584.

[15] Athay, T., V. Sherket, R. Podmore, S. Virmani and C. Puech. "Transient Energy Stability Analysis." *Proc. Conference on Systems Engineering for Power: Emergency Operating State Control,* Davos, Switzerland, 1979. U.S. Dept. of Energy Publication No. CONF-790904-PL, Section IV.

[16] Kakimoto, N., Ohsawa, Y. and Hayashi, M. "Transient Stability Analysis of Electric Power Systems via Lur'e Type Lyapunov Function." *Proceedings of IEE Japan* 98 (May/June 1978): 63-78.

[17] Fouad, A. A. and S. E. Stanton. "Transient Stability Analysis of a Multimachine Power System. Part I: Investigation of System Trajectory; and Part II: Critical Transient Energy." *IEEE Trans.* PAS-100 (August 1981):3408-3424.

[18] Fouad, A. A., K. C. Kruempel, K. R. C. Mamandur, S. E. Stanton, M. A. Pai and V. Vittal. "Transient Stability Margin as a Tool for Dynamic Security Assessment." *EPRI Report EL-1755*, March 1981.

[19] Fouad, A. A., V. Vittal and T. Oh. "Critical Energy for Transient Stability Assessment of a Multimachine Power System." *IEEE Trans.* PAS-103 (1984): 2199-2206.

[20] Chiang, H. D., F. F. Wu and P. P. Varaiya. "Foundations of Direct Methods for Power System Transient Stability Analysis." *IEEE Trans. on Circuits and Systems*, CAS-34, February 1987: 160-173.

[21] Vittal, V. "Power System Transient Stability Using the Critical Energy of Individual Machines." Ph.D. Dissertation, Iowa State University, Ames, Iowa, 1982.

[22] Michel, A. N., A. A. Fouad and V. Vittal. "Power System Transient Stability Using Individual Machine Energy Functions." *IEEE Trans.* PAS-30 (May 1983): 266-276.

[23] Rajagopal, S. "Application of the Transient energy Function Method to Stressed Large-Scale Power Systems." Ph.D. Dissertation, Iowa State University, Ames, Iowa, 1987.

[24] Carvalho, V. F., M. A. El-Kady, E. Vaahedi, P. Kundur, C. K. Tang, G. Rogers, J. Libaque, D. Wong, A. A. Fouad, V. Vittal and S. Rajagopal. "Direct Analysis of Transient Stability for Large Power Systems." *EPRI Report EL-4980*, December 1986.

[25] Nodehi, K. "Incorporating the Effect of Exciter in the Transient Energy Function Method" Ph.D. Dissertation, Iowa State University, Ames, Iowa, 1987.

[26] Fouad, A. A., V. Vittal, Y. X. Ni, H. R. Pota, K. Nodehi and T. K. Oh. "Extending Applications of the Transient Energy Function Method." EPRI Report No. EL-5215, September, 1987.

[27] Oh, T. "Correlation of the Transient Energy Margin to Out-of-Step impedance relay operation." Ph.D. Dissertation, Iowa State University, Ames, Iowa, 1986.

[28] Concordia, C. "Representation of Loads" *IEEE Power Engineering Society 1975 Winter Meeting Paper, Symposium on Adequacy and Philosophy of Modeling: Dynamic System Performance*, 1975.

[29] Athay, T. and D. I. Sun. "An improved Energy Function for Transient Stability Analysis." *Proc. of IEEE International Symposium on Circuits and Systems*, Chicago, April 1981.

[30] Pai, M. A., K. R. Padiyar and C. Radhakrishna. "Transient Stability Analysis of Multimachine AC/DC Power Systems Via Energy Function Method." *IEEE Trans. on Power Apparatus and Systems*, PAS-100, December 1981: 5027-5035.

[31] Sastry, H. S. Y. "Application of Topological Energy Functions for the Direct Stability Evaluation of Power Systems." Ph.D. Dissertation, IIT Kanpur, India, May 1984.

[32] Anderson, P. M. and Fouad, A. A. *Power System Control and Stability.* Vol. 1. Ames, Iowa: The Iowa State University Press, 1977.

[33] Lightfoot, S. R., J. D. Whitaker and D. L. Brown. "EPRI Transient-Midterm Stability Program Support Software Technical Guide." *EPRI Report EL-600*, June 1979.

[34] Tinney, W. F. and Powell, W. L. "The REI Approach to Power Network Equivalent." Proceedings of the 1977 PICA, pp. 314-320, Toronto, Canada, May 1977.

[35] Porter, B. and Crossley, R. *Modal Control Theory and Applications.* London, UK: Taylor and Francis Ltd., 1972.

[36] Verghese, G. C., I. J. Perez-Arriaga, F. C. Schweppe and K. W-K. Tsai. "Selective Modal Analysis in Power Systems." *EPRI Report EL-2830*, January 1983.

[37] Kailath, T., *Linear Systems.* Englewood Cliffs. N.J.: Prentice-Hall, Inc., 1980.

[38] Zadeh, L. A. and Desoer, C. A. *Linear System Theory the State Space Approach.* New York: McGraw-Hill Book Company, Inc., 1963.

[39] Litz, L. "Order Reduction of Linear State Space Models via Optimal Approximation of the Nondominant Modes." Large Scale Systems 2. Amsterdam: North-Holland Publishing Company, 1981, pp 171-174.

[40] Berggren, B. "Transient Stability Behavior in a Stressed Power System." M.S. Thesis, Iowa State University, Ames, Iowa, 1988.

[41] Vittal V., S. Rajagopal, A. A. Fouad, M. A. El-Kady, E. Vaahedi and V. Carvalho. "Transient Stability Analysis of Stressed Power Systems Using the Energy Function Model." *Proc. 1987 Power Industry Computer Applications Conference*, May 1987: 253-258.

9 ACKNOWLEDGMENTS

I am very grateful to my major professor Dr. V. Vittal for giving his constant attention and time to this research work. His deep interest and encouragement were of immense help in pursuing this research.

I would especially like to thank Dr. A. A. Fouad for his invaluable guidance and encouragement. His constant reminder to view the system from a physical aspect was of great help in formulating and solving this research problem.

I am thankful to Dr. K. C. Kruempel for exposing me to the special computer programming skills required for power system analysis and for helping me with the various computer programs. Special thanks are extended to Dr. T. Georgiou and Dr. R. K. Miller for their enthusiastic participation in my graduate committee.

I would like to thank my parents for their constant encouragement and moral support throughout my graduate program.

I take this opportunity to thank my fellow graduate students for their friendship and moral support, and for the good times we shared together. Thanks are also extended to the secretaries of the Electrical Engineering and Computer Engineering department.

I am indebted to the Electrical Engineering and Computer Engineering department at Iowa State University for their financial assistance.

10 APPENDIX

A Newton-Raphson approach developed in [33] is used to iteratively obtain the solutions to equation (3.2).

The equation (3.2) is represented in the rectangular form as

$$\left[\underline{I} \right] = \left[\mathbf{Y} \right] \left[\underline{V} \right] \tag{10.1}$$

where

$$\begin{aligned} I_i &= c_i + jd_i, \qquad i = 1,2,\ldots,n \\ Y_{ij} &= G_{ij} + jB_{ij}, \quad i,j = 1,2,\ldots,n \\ V_i &= e_i + jf_i, \qquad i = 1,2,\ldots,n. \end{aligned}$$

Expanding the above equation in terms of the rectangular coordinates, we get

$$c_i + jd_i = \sum_{j=1}^{n} \left(G_{ij} + jB_{ij}\right)\left(e_j + jf_j\right) \qquad i = 1,2,\ldots,n \tag{10.2}$$

or (10.3)

$$c_i = \sum_{j=1}^{n} \left(G_{ij}e_j - B_{ij}f_j\right)$$

$$d_i = \sum_{j=1}^{n} \left(B_{ij}e_j + G_{ij}f_j\right) \tag{10.4}$$

The unknown vector $\underline{x} = [e_1, e_2, \ldots, e_n, \quad f_1, f_2, \ldots, f_n]^T$. We want solutions to

the equations

$$\underline{F}(\underline{x}) \;=\; \underline{y} \tag{10.5}$$

where

$\underline{y} = [d_1, d_2, \ldots, d_n,\;\; c_1, c_2, \ldots, c_n]$

$$\begin{aligned} F_i(\underline{x}) &= \sum_{j=1}^{n} \left(B_{ij} e_j + G_{ij} f_j \right), \quad i = 1, 2, \ldots, n \\ &= \sum_{j=1}^{n} \left(G_{(i-n)} e_j - B_{(i-n)} f_j \right), \quad i = n+1, \ldots, 2n \end{aligned} \tag{10.6}$$

The iterative solution is set up as

$$\underline{y} - \underline{F}(\underline{x}) \;=\; \mathbf{J}\underline{x} \tag{10.7}$$

where

$$\mathbf{J} = \begin{bmatrix} B_{11} & B_{12} & \cdots & B_{1n} & G_{11} & G_{12} & \cdots & G_{1n} \\ \vdots & \vdots & \vdots & \vdots & \vdots & \vdots & \vdots & \vdots \\ B_{n1} & B_{n2} & \cdots & B_{nn} & G_{n1} & G_{n2} & \cdots & G_{nn} \\ G_{11} & G_{12} & \cdots & G_{1n} & -B_{11} & -B_{12} & \cdots & -B_{1n} \\ \vdots & \vdots & \vdots & \vdots & \vdots & \vdots & \vdots & \vdots \\ G_{n1} & G_{n2} & \cdots & G_{nn} & -B_{n1} & -B_{n2} & \cdots & -B_{nn} \end{bmatrix}$$

The updated $x_i^{(k+1)} = x_i^{(k)} + \Delta x_i^{(k)}$ is obtained, the new injected currents are calculated using equation (3.3), and the solution is repeated. The procedure is continued until two successive values for each x_i differ only by a specified tolerance.